DEVELOPMENT OF HIGH TEMPERATURE RESONANT ULTRASOUND SPECTROMETER

A Thesis

by

DONGGI HA

Submitted to the Office of Graduate and Professional Studies of
Texas A&M University
in partial fulfillment of the requirements for the degree of

MASTER OF SCIENCE

Chair of Committee,	Radovic, Miladin
Committee Members,	Ross, Joseph H
Committee Members,	Karaman, Ibrahim
Head of Department,	Karaman, Ibrahim

May 2021

Major Subject: Material Science and Engineering

ABSTRACT

Resonant Ultrasound Spectroscopy (RUS) is an experimental technique that can provide a full set of elastic constants of a solid from a single measurement as well as ultrasonic attenuation in solids. This technique is based on measuring a mechanical resonance spectrum of a sample of known geometry, dimensions and mass that can be used to determine elastic constants of the solid with known geometry, dimensions and mass. Currently, all commercially available RUS system can be used only for measurements at room temperatures, while some custom-made systems allow measurements at temperatures up to 1100 ˚C.

In this study, a high temperature RUS system has been developed for measuring elastic moduli of solids from room temperature up to 1600 ˚C in controlled environments. Elastic moduli of different materials were obtained using the developed high temperature RUS and were statistically analyzed and systematically compared to the values obtained using commercially available or other customized high temperature techniques. The newly developed RUS apparatus overcomes current limitations of high temperature RUS systems and further extends measurements of elastic constants in a wider range of temperature and sample size. In addition, the developed RUS system is more user friendly and allows easier maintenance and use than other high temperature RUS systems.

ACKNOWLEDGEMENTS

I would like to appreciate for my academic mentors Dr. Radovic as well as Dr. Ross and Dr. Karaman who guided me through my academic research and personal growth over the last two years. Moreover, I would like to thank all my mentors for giving me opportunity to do academic research that I was passionate about.

Additionally, I would like to thank Lei Xue who helped me with Infrared(IR) experiment and thank to all my peers, colleagues and Materials Science and Engineering (MSEN) faculty and staff for making my time at Texas A&M University a wonderful experience. I also want to express gratitude to machine shop in Materials Science and Engineering and Chemistry departments that provided a materials and manufacturing for my academic research.

Finally, thanks also to Kurt J. Lesker, Micropyretics Heaters International Inc., Magnaflux and Kyocera for their help in selecting, designing and building components needed for building Resonant Ultrasound Spectrometer as a part of my academic research.

CONTRIBUTORS AND FUNDING SOURCES

Contributors

This work was supervised by a M.S. committee consisting of Dr. Miladin Radovic and Dr. Karaman of the Department from Materials Science and Engineering and Dr. Joseph Ross from the Department of Physics.

The Chamber bench described in Section 3.1 was designed and built by Michael Elverud at the Materials Science and Engineering. All other work conducted for the dissertation was completed by the student independently.

Funding Source

This work was supported by a U.S. National Science Foundation through MRI grant (Award: DMR-1726887), which provided the funding for the research.

NOMENCLATURE

RUS	Resonant Ultrasound Spectroscopy
NDT	Non-Destructive Technique
HT-RUS	High Temperature Resonant Ultrasound Spectroscopy
σ_{ij}	Stress
ε_{kl}	Strain
C_{ijkl}	Elastic Constants
E	Young's Modulus
G	Shear Modulus
v	Speed of Sound
p	Density
Q^{-1}	Ultrasonic attenuation
FWHM	Full width at half maximum
ω_{k0}	Frequency related to k-th eigenmode
L	Lagrangian
KE	Kinetic Energy
PE	Potential Energy
V	Volume
μ	i_{th} Component of the Displacement Vector
ω	Angular frequency
t	time
$\alpha_{i\lambda}$	Expansion Coefficient

ϕ_λ	Basis Function
w	Weighting factor
f_i	Calculated frequency
g_i	Measured Frequency
RMS	Root-Mean-Square
ID	Inner Diameter
OD	Outer Diameter
Al_2O_3	Aluminum Oxide
PID	Proportional, Integral, Derivative
Si_3N_4	Silicon Nitride
TaC_{3-x}	Tantalum Carbide
SMA	Sub-miniature coaxial cable connector

TABLE OF CONTENTS

Page

ABSTRACT ii
ACKNOWLEDGEMENTS iii
CONTRIBUTORS AND FUNDING SOURCES iv
NOMENCLATURE v
LIST OF FIGURES ix
LIST OF TABLES xi
1. INTRODUCTION 1
1.1 Motivation 1
1.2 Research Objective 3
2. LITERATURE REVIEW 4
2.1 Background 4
2.2 Review of HT-RUS system 7
2.3 Theory of Resonant Ultrasound Spectroscopy 9
3. DESIGN AND FUNCTIONAL DECOMPOSITION OF NEWLY DEVELOPED HT-RUS 14
3.1 Functional chart of the components 14
3.2 Functional decomposition and design of HT-RUS 14
3.3 Description of the developed High-Temperature RUS 25
3.4 Specifications of the instrument to build 32
3.5 Experimental procedure 33
4. TESTING OF THE DEVELOPED HT-RUS APPARATUS 36
4.1 Vacuum system testing 36
4.2 Culling water circulation system 38
4.2 Infrared (IR) testing of HT-RUS setup 38
4.3 Comparison of resonant spectra collected using HT-RUS and commercial apparatus at room temperature. 40
4.4 Elastic moduli of Aluminum Oxide determined using developed HT-RUS 43
4.5 Silicon Nitride 47
4.6 Tantalum Carbide 51
5. CONCLUSION AND FUTURE WORK 54
REFERENCE 57

APPENDIX A 57
Technical drawings 62
APPENDIX B 70
User and maintenance manual 70

LIST OF FIGURES

Page

Figure 1. Schematic of RUS system (a) tripod setup and (b) tip-to-tip setup 8

Figure 2. Functional chart of the HT-RUS components..... 13

Figure 3. Major components for the designed HT-RUS system 16

Figure 4. Schematic of major components of the stage for tripod measurement setup in the developed High temperature RUS where (a) is transducer holder, (b) is a bottom plate, and (c) is a furnace holder 17

Figure 5. Schematic of the transducer holder with cooling channels..... 19

Figure 6. Schematic of the bottom plate with heat shield plate and transducer holders 20

Figure 7. Box chamber assembly with all the ports 22

Figure 8. High Temperature RUS system (a) Inside of the chamber
(b) Outside of the chamber..... 25

Figure 9. (a) Stage for tripod measurement setup with the furnace, (b) Bottom plate with furnace holder and heat shield located in the vacuum chamber..... 26

Figure 10. Chamber frame with a vacuum/environmental chamber (a) front view
(b) bottom view 28

Figure 11. Vacuum pump connection for HT-RUS 29

Figure 12. Multidimensional algorithm of the RUS system [12]..... 31

Figure 13. Screen shot of RUSpec 31

Figure 14. Newly developed HT-RUS tripod setup with transducer holder 35

Figure 15. Vacuum gauge of pressure inside the chamber..... 37

Figure 16. Infrared images of the temperature distribution during heating
HT-RUS furnace at 1600 ºC (a) Transducer temperature
(b) Furnace temperature 39

Figure 17. Resonant spectra of Al_2O_3 collected using developed HT-RUS and commercial setups at room temperature..... 41

Figure 18. Resonant spectra of Al_2O_3 at different temperature 43

Figure 19. Young's and Shear modulus of Al_2O_3 sample determined using developed HT-RUS 44

Figure 20. Comparison of normalized Young's and shear modulus of Al_2O_3 at different temperatures, obtained using developed HT-RUS and reported Goto and Anderson [34] and Watchtman and Lam [35] 45

Figure 21. Resonant spectra of Si_3N_4 at different temperature 48

Figure 22. Young's and Shear moduli of Si_3N_4 determined using developed HT-RUS 49

Figure 23. Young's modulus of Si_3N_4 comparison with literature value [39] 50

Figure 24. Resonant spectra of ζ-Ta_4C_{3-x} at different temperature 51

Figure 25. Young's and shear moduli of ζ-Ta_4C_{3-x} as a function of temperature between room temperature and 1200 ºC 53

LIST OF TABLES

Table 1. Specification of the Newly developed HT-RUS component 32

Table 2. Resonant peak and frequency peak collected from using developed HT-RUS and commercial setup 42

Table 3. Room temperature elastic moduli and Possion's ratio of Al_2O_3 determined from resonant spectra collected using developed HT-RUS and commercial setup 42

Table 4. A full set of elastic constant of ζ-Ta_4C_{3-x} at room temperature [40] 52

1. INTRODUCTION

1.1 Motivation

Mechanical properties of any material, such as stiffness, yield strength, tensile strength, and ductility, are crucial for their use, especially in different structural applications. These properties can determine the range of usefulness of the particular component, such as load bearing capability, deformability, service life, etc. Therefore, to utilize a material appropriately to its full capacity for a particular application, it is important to know and understand its mechanical properties. Among those mechanical properties, elastic constants are considered to be the most fundamental ones. Elastic constants, as the second derivative of the free energy with respect to strain, not only express a relation between the stress and the strain of a material, but also provide information about atomic bonding in a solid. However, in order to obtain a full set of elastic constants of any solid with lower symmetry requires numerous samples to be tested using conventional techniques, which is usually extremely time-consuming process, especially when testing is done at various temperatures.

Ultrasonic techniques, especially pulse-based ones, are the most broadly used methods to measure elastic constants. In pulse-echo technique, the transmitter generates ultrasonic pulsed waves that are further transmitted to the specimen reflected from the opposite surface of the sample, and then detected by the receiver. Elastic moduli can be obtained in this case by measuring the time of flight to calculate sound speed in a particular solid of known thickness (dimensions), that can be afterwards directly related do the elastic constants of the solid. In addition, pulse-echo systems are also able to detect defects in materials through an ultrasonic pulsed wave, and thus it is widely used as non-destructive technique (NDT). However, only

one component of the elastic tensor at a time can be measured using this pulse-based methods [1].

The other ultrasonic technique involves ultrasonic resonant ultrasound spectroscopy (RUS). Unlike in the case of the pulse-echo system, RUS can provide a full set of elastic constants in a single measurement [2]. In addition, RUS technique has a tendency of having a better reproducibility and accuracy of the results, when compared to other techniques. The accuracy comparison between pulse-echo and resonance system has been performed at Los Alamos National Laboratory and the results showed that RUS has measurements error of only 0.05% while pulse-echo method usually show error of ≥0.1%. High accuracy and an ability to obtain all elastic properties on small specimens with just one experiment are the key significant advantages of using RUS when compared to other techniques for measurements of solids [3].

Currently, there is only one commercially available RUS system (Quasar RUSpec system, Magnaflux, Glenview, IL). However, this commercial system is limited to only room temperature measurements. Recently, a few custom-made RUS systems have been developed for measurement at temperatures up to 1100 ◦C in controlled environments and, but no RUS system has been built that is capable of measurements above that temperature. A development of such a RUS system, that is applicable to even higher temperature, will provide a powerful new method to obtain elastic properties of materials especially materials to be used in extreme conditions such as hypersonic flight, nuclear power reactors, rocket engines, etc.

1.2 Research Objective

The main objective of this research is to design and build a new High-Temperature Resonant Ultrasound Spectrometer (HT-RUS) capable of measuring a full set of elastic constants of solids at temperatures ranging from room temperature up to 1600 ˚C in a controlled environment. To achieve this objective, the following requirements needs to be satisfied.

- This instrument should be user friendly and allow easy maintenance and use.
- Vacuum pressure in the chamber should meet our desired condition to min. $10^{-3} torr$
- Transducer temperature should be below 50˚C while running experiment at the highest temperature to avoid their damage
- Newly developed HT-RUS system should provide the same results as commercially available RUS system at the room temperature.
- Functional testing of a newly developed HT- RUS has to be carried out at different temperatures and environments (vacuum, inert gas at different pressures and flow rate, etc.)
- Last but not least, elastic constants of various materials (such as Al_2O_3 , Si_3N_4 , TaC_{3-x},etc.) should be measured at different temperatures using developed HT-RUS and compared to the results available in the literature

2. LITERATURE REVIEW

2.1 Background

The Resonant Ultrasound Spectroscopy (RUS) is a simple and inexpensive laboratory experimental technique that relies on various information collected from the different natural modes of vibration of solids [4]. This technique allows determination of elastic moduli of a solid from resonance frequencies of various natural modes of vibrations from the single vibration spectra of a freely suspended solid. RUS have been used since 1964 to measure the elastic moduli of the samples with the spherical shape [5]. Since then, researchers have been constantly improving this technique for measurements using samples with various geometries, such as solid cubes, cylinders, discs and parallelepipeds [6-11]. In addition, early RUS measurements required numerical methods and calculations by hand to determine elastic constants from the measured resonant frequencies from the resonance spectra, which consumed immense amount of time and usually resulted in large errors. However, computer-based calculations developed in 1970s to resulted in accurate and faster analysis of the resonant spectra to obtain elastic constants.

Elastic constants are some of the most fundamental properties of any solid. The elastic response of a solid is governed by material's interatomic forces and curvature of the potentials, and is described by the full set of 81 independent elastic constants for generally anisotropic material [12]. Elastic constants are also related to thermal properties of the solid through Debye theory [4, 13]. Therefore, elastic constants can be crucial to understand fundamental physical properties of any solid.

From the engineering point of view, elastic constants are important since they relate forces acting on the solid and its deformation according to:

$$\sigma_{ij} = C_{ijkl}\varepsilon_{kl} \tag{1}$$

where σ_{ij} and ε_{kl} are the stress and strain tensors respectively, and C_{ijkl} are 81 elastic constants [14, 15]. Equation (1) is also known as generalized Hooke's law. In the case of triclinic symmetry, the number of independent elastic constants can be reduced to 21. In addition, an isotropic material, elastic constants are only required two independent elastic constants C_{11} and C_{44}, or more commonly Young's modulus, E, and Shear modulus, G, [2].

Considering scientific and engineering importance of elastic constants various theoretical and experimental methods have been developed to determine elastic constants of solids including ab initio calculations, and experimental static, such as quasi-static, and dynamic experimental techniques. The selection of experimental techniques depends on the size of the sample, structure of the sample, its composition, and required testing condition, among others. However, among all experimental methods, non-destructive ultrasonic techniques are praised not only because of their non-destructive nature, but also due to their high efficiency and accuracy [16, 17]. Currently, there are two ways to measure elastic constants using ultrasound pulse-echo and RUS. In pulse-echo technique, speed of sound is utilized which rely on material density and its elastic constants according to

$$v = \sqrt{\frac{C_{ij}}{p}} \tag{2}$$

where v is the speed of sound, C_{ij} is the elastic constant relevant to v, and p is the density of material. This technique enables to obtain elastic constants of single crystals in different directions with very high precision, as well as those of on quasi-isotropic polycrystalline aggregates [18]. However, the major drawbacks of this techniques are that it requires multiple samples to obtain a full set of elastic constants for single crystals and cannot be used at high temperatures.

On the other hand, another ultrasonic technique, namely Resonant Ultrasound Spectroscopy (RUS) is a simple and inexpensive laboratory experimental technique that relies on

a reflection of various information emerged by the natural mode of vibration of solids [4]. RUS is based on measuring mechanical resonances of solid object which can be further used to determine a full set of elastic constants from a single measurement.

RUS utilizes free vibration frequencies of natural vibrational modes of the solids which depends on density and dimensions of the material, and its full set of the elastic constants using samples with broad range of sizes, from seamless with dimensions of 1 mm to couple of centimeters or even larger. Moreover, RUS provides repeatability and accuracy when compare to other ultrasonic techniques [19]. Although this ultrasonic technique is valuable, there are certain limitations [20]. First, RUS requires use of piezoelectric transducers which are not suitable at high temperature, and thus RUS has been limited to measurements below approximately 40^{o}C. Furthermore, the sample preparation is quite intense, especially for low-symmetry crystals, because samples have to have a perfect geometry.

In addition, RUS also allows measurement of ultrasonic attenuation (Q^{-1}) which is related to the energy absorbed by various inelastic physical processes during mechanical vibration of the sample, and can be determined as:

$$Q^{-1} = \frac{\Delta\omega_k}{\omega_{k0}} \tag{3}$$

where $\Delta\omega_k$ is the full width at half maximum, FWHM, of the k_{th} eigenmode and ω_{k0} is the frequency related to k_{th} eigenmode [4].

2.2 Review of HT-RUS system

Although commercially available RUS systems, such as that by Quasar RUSpec system, Magnaflux, Glenview, IL, are limited only to measurements at room temperatures. Over the past several years a very few systems has been custom made for measurements at extremely low and high temperature as well as in the high magnetic fields [14, 21, 22] [12, 23-27]. However, measurements of elastic properties at elevated temperatures using RUS are still very rare [28] and they have been all limited to maximum 1100°C for the several reasons. First, the strength of the acoustic resonance of most materials are weak at elevated temperatures and large broadening of the resonant peaks due to attenuation is usually observed. Second, piezoelectric transducers used to generate and receive signal in RUS must be kept well below their curie temperatures [28-30]. Third, high temperature RUS measurements are extremely sensitive at eventual oxidation of samples.

In general, RUS is performed using two experimental setups. In tripod setup, three piezoelectric transducers are used to hold the free suspended sample, while in tip-to-tip system sample is slightly clamped between two transducers. In tripod RUS configuration, one of the transducers generates an elastic wave of constant amplitude, the other two transducers receive the resonance signal as it is shown in **Figure 1.a**. The other common system, tip-to-tip system shown in **Figure 1.b**, sample is placed between two transducers perpendicularly touching the corner edge of the sample. This system is more challenging for use than the tripod setup because small pressure must be applied to the sample since sample to keep it clamped between two transducers. In addition, it is difficult to control pressure induced on the sample during high-temperature measurements, due to thermal expansions of the sample and the setup. However, tip-to-tip system is preferred for testing very small samples.

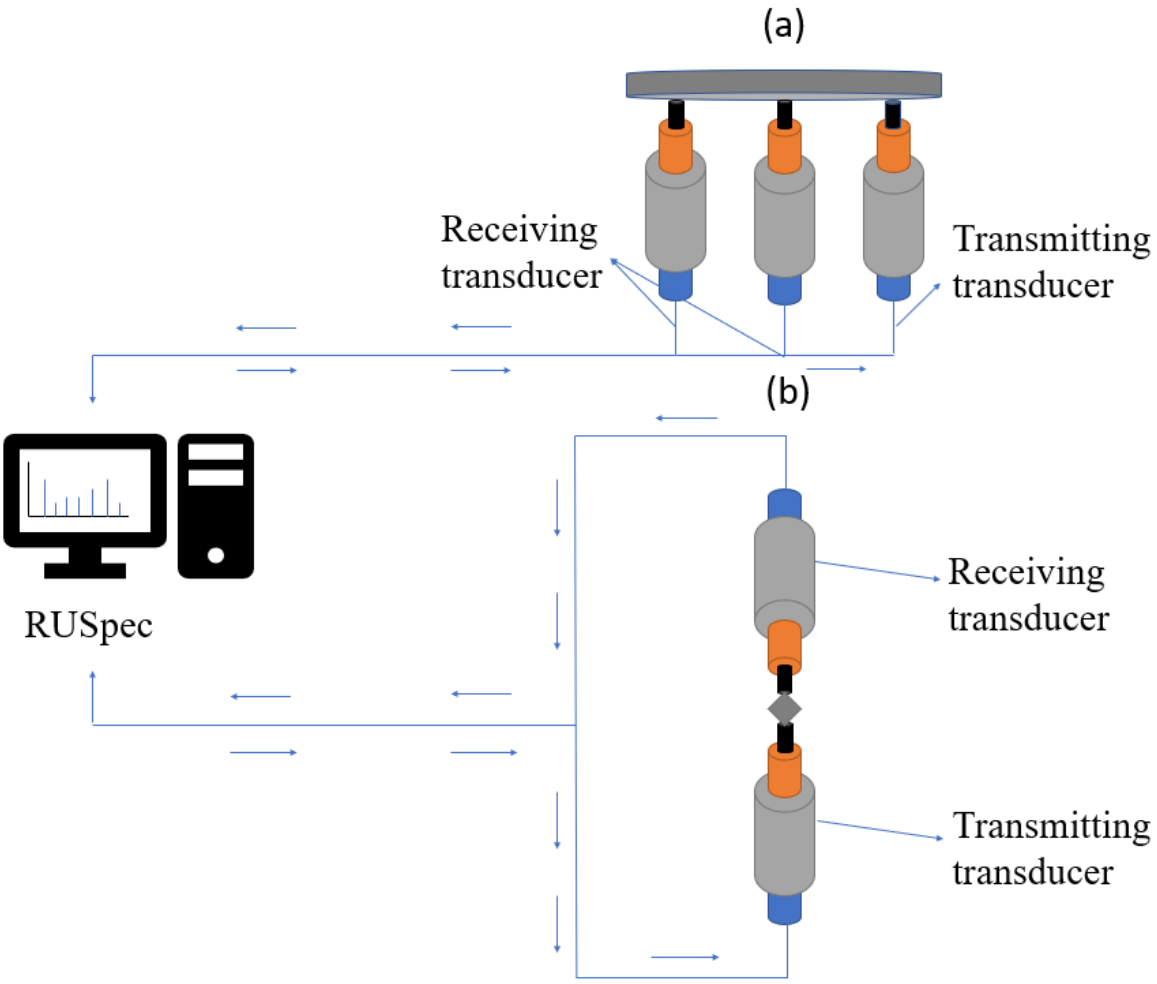

Figure 1. Schematic of RUS system (a) tripod setup and (b) tip-to-tip setup

2.3 Theory of Resonant Ultrasound Spectroscopy

RUS utilizes mechanical resonance spectrum to determine elastic constants of the solid by solving elastic wave equation for a sample of known geometry, dimensions, and mass, that is referred to a inverse problem. In contrast, a forward problem consists of calculation eigen-frequencies for given crystal symmetry, shape, elastic constants, and density [13, 21]. In the case of solving a forward problem for arbitrarily shaped sample, the following Lagrangian equation can be used [4] :

$$L = \int_V (KE - PE) dV \tag{4}$$

where KE and PE are kinetic potential energy, respectively given as:

$$KE = \frac{1}{2} p\omega^2 \mu_i^2 \tag{5}$$

$$PE = \frac{1}{2} C_{ijkl} \mu_{i,j} \mu_{k,l} \tag{6}$$

where C_{ijkl} is elastic tensor, V is volume of the sample, p is density, μ is the i_{th}component of the displacement vector. Note that the time dependence of the displacement is assumed to be $e^{i\omega t}$ where ω is angular frequency and t is the time.

To find the minimum of the Lagrangian we, convert μ_i to $\mu_i + \delta\mu_i$ and calculate the variation in L (δL) as:

$$\mathrm{L} + \delta\mathrm{L} = \int_V [\frac{1}{2} \sum_i p\omega^2 (\mu_i + \delta\mu_i)^2 - \sum_{i,j,k,l} C_{ijkl} \frac{\partial(\mu_i + \delta\mu_i)}{\partial x_j} \frac{\partial(\mu_k)}{\partial x_l}] \mathrm{dV} \tag{7}$$

then, integrate Eq. (7) to get the elastic wave equation and free-surface boundary condition in the following from:

$$\delta\mathrm{L} = \int_V \{\sum_i [\rho\omega^2 \mu_i + \sum_{i,j,k,l} C_{ijkl} \frac{\partial^2 \mu_k}{\partial x_j \partial x_l}] \delta\mu_i\} \mathrm{dV} - \int_s \{\sum_i [\sum_{j,k,l} \vec{n_j} C_{ijkl} \frac{\partial \mu_k}{\partial \mu_l}] \delta\mu_i\} ds \tag{8}$$

$$\rho\omega^2 \mu_i + \sum_{i,j,k,l} C_{ijkl} \frac{\partial^2 \mu_k}{\partial x_j \partial x_l} = 0 \tag{9}$$

$$\sum_{j,k,l} \overrightarrow{n_j} C_{ijkl} \frac{\partial \mu_k}{\partial \mu_l} = \sum_j n_j \sigma_{ij} = 0 \quad (10)$$

where Equations (9) and (10) are expression for elastic wave equation and free-surface boundary condition respectively. Note that σ_{ij} is the ij_{th} component of the stress tensor. The discrete set of normal mode frequencies of free vibrations of the system is achieved when the set of μ_i satisfies these conditions [4].

Continuously, Ritz method is applied to expand displacements vector in complete set of basis function according to [4]:

$$\mu_i = \sum_i \alpha_{i\lambda} \phi_\lambda \quad (11)$$

where $\alpha_{i\lambda}$is the expansion coefficients and $\phi_\lambda$is the basis function. The ϕ_λ are usually chosen by the shape of the sample. In particular, it is necessary to be able to integrate the basis functions and their derivatives over the volume of the sample. For parallelepipeds, Legendre polynomials [21, 22] is usually a useful choice for ϕ_λ as a series expansion with x,y,z:

$$\phi_\lambda = x^l y^m z^n \quad (12)$$

where l, m, and n integers that can also used for a variety of shapes [31]. As in equation (11), each of the three components of the displacement is expanded and each has its unique set of coefficients of expansion. Substitution of equation (11) of the Lagrangian gives:

$$L = \int_v \frac{1}{2} [\sum_{i,i',\lambda,\lambda^i} \delta_{ii'} \rho \omega^2 \alpha_{i\lambda} \alpha_{i'\lambda'} \phi_\lambda \phi_{\lambda'} - \frac{1}{2} \sum_{i,j,k,l,\lambda,\lambda'} C_{ijkl} \alpha_{i\lambda} \alpha_{i'\lambda'} \frac{\partial \phi_\lambda}{\partial x_j} \frac{\partial \phi_{\lambda'}}{\partial x_i}] dV \quad (13)$$

where the summations on λ and λ' are from 1 to N (l+m+n < N,). This can be rewritten more compactly as:

$$L = \frac{1}{2} \omega^2 \vec{\alpha}^T E \vec{\alpha} - \frac{1}{2} \vec{\alpha}^T \boldsymbol{\Gamma} \vec{\alpha} \quad (14)$$

in which integrals appearing in equation (13) are the elements of matrices E and **Γ** and where α is a vector with α_i whose transpose is α^T. Applying to original Lagrangian form (L) and derivating

of the Lagrangian with respect to the expansion coefficients set to be zero gives as a result a generalized eigenvalue equation as follows:

$$\omega^2 E\vec{\alpha} = \Gamma\vec{\alpha} \tag{15}$$

Once Lagrangian become stationary, eigenvalues and eigenvectors are provided giving the free-oscillation frequencies of the solid and its physical displacements when oscillating at resonant frequencies [13, 14, 32, 33].

Although the measurement of the resonance frequencies of the body is a significant achievement, one has to solve inverse problem to calculate elastic moduli by from measured resonance frequencies of the body considering its mass, dimensions, orientation angles and elastic moduli, to fully utilize RUS. However, the solution of the forward problem is the key for the solution of this inverse problem. The inverse problem utilizes a standard non-linear least-squares algorithm (Levenburg-Marquardt algorithm). In order to determine the "best values" for the parameters in elastic wave equation, the first step is to apply a figure of merit, F, which provides a measure of how well the calculated and measured resonance frequencies agree [4, 13]:

$$F = \sum_{i=1}^{N} w_i (f_i - g_i)^2 \tag{16}$$

where w is a weighting factor for frequency *i*, and f_i and g_i are the *i*-th calculated and measured frequencies, respectively. The function defined in Eq. (16) is presumed to have a minimum when the correct set of parameters is reached. If the current set of parameters, $x_{\alpha 0}$, is close enough to the correct set of parameters, x_α", an expansion of equation (17) to the second order will provide a close approximation to the function F as:

$$\mathrm{F}(\chi) = \mathrm{F}\,(\,x_\alpha) + \left(\frac{\partial F}{\partial x_\alpha}\right)_{x_{\alpha 0}} (x_\alpha - x_{\alpha 0}) + \frac{1}{2}\left(\frac{\partial^2 F}{\partial x_\alpha \partial x_\beta}\right)_{x_{\alpha 0}\, x_{\beta 0}} (\chi_\beta - \chi_{\beta 0}) + \cdots \tag{17}$$

The repeated indices, α and β, are to be summed over the number of parameters, M, which are to be varied. When χ is the correct set of parameters, F will be at the minimum and derivation of

equation (17) with each of the parameters, x_α will yield zero. Thus, a set of M equations is written as:

$$\left(\frac{\partial F}{\partial x_\alpha}\right)_{x_{\alpha 0}} + \left(\frac{\partial^2 F}{\partial x_\alpha \partial x_\beta}\right)_{x_{\alpha 0}\, x_{\beta 0}} (\chi_\beta - \chi_{\beta 0}) = 0 \tag{18}$$

Then solve for x_α is given as

$$x_\alpha = x_{\alpha 0} - A_{\alpha\beta}^{-1} B_\beta \tag{19}$$

where the derivatives from equation (18) are the elements of the matrices A and B in equation (19). The Equation (19) then, gives a means of calculating a new set of parameters, based on the current parameters, which provides a better fit between measured and calculated frequencies. As solving iteratively using these new parameters, the value of root-mean square (RMS%) difference among frequencies for the first usually 40 measured and calculated modes usually has to be reach value less than 0.4% to achieve iteratively acceptable value of particular set of parameters, especially elastic constants. This process is the key algorithm to obtain accurate determination of the elastic constants using RUS. Described algorithm for solving inverse problem is utilized in the commercially available software RUSpec (Quasar RUSpec system, Magnaflux, Glenview, IL) for fitting measured resonant frequencies to obtain full set of elastic constants, and this software is used in conjunction with developed HT-RUS system to analyze experimental results.

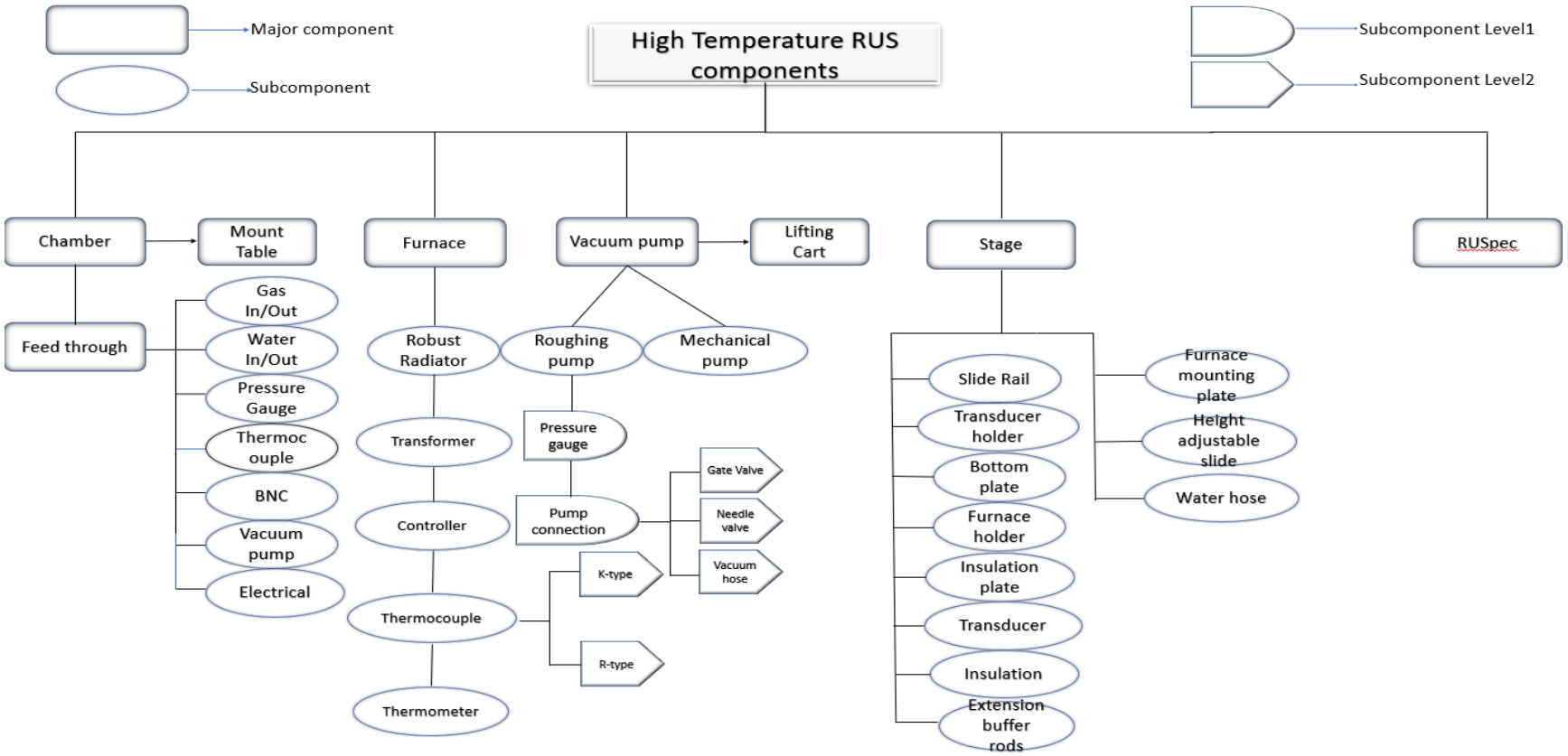

Figure 2. Functional chart of the HT-RUS components

3. DESIGN AND FUNCTIONAL DECOMPOSITION OF NEWLY DEVELOPED HT-RUS

3.1 Functional chart of the components

In order to overcome previously described potential limitations in operation of the HT-RUS, first the function of each components is summarized as shown in **Figure 2** and all conditions needed for their proper operations are analyzed in the reminder of this section.

3.2 Functional decomposition and design of HT-RUS

The RUSpec signal generator generates a signal to the tripod stage with three transducer which is located inside of the vacuum chamber with tripod stage in order to determine resonant spectrum of the sample resting on the tips of the extension rods attached to the transducers. The sample sitting on the tips of the extension rod needs to be placed in the furnace cable of reaching 1600^{o}C. Proper furnace operation requires transformer and a controller with thermometer. Two types of thermocouple K-type and R-type have to be used at two different position; R-type inside of the furnace to monitor temperature in the furnace, and K-type is near the transducer to detect temperature of the transducers. Also, an additional overheating thermometer (R-type) is to control the temperature of the furnace.

Entire measuring stage with furnace has to be located in the vacuum/environmental for testing samples sensitive to oxidation or any chemical interaction with air at elevated temperature. The chamber needs to be connected with vacuum pump system and gas supply system. The vacuum pump system consists of two separate pumps, a roughing pump and a turbo pump, in this system.

To achieve a proper test environment of the chamber, roughing pump is needed to first reach pressure of $10^{-2}\ torr$, then the turbo pump is needed to reach a pressure of minimum $10^{-4}\ torr$ at the pump exit. Once a proper vacuum pressure is achieved, evacuation of the chamber needs to be stopped, and of needed chamber should be backfield with flowing inert gas at the pressure slightly above atmospheric pressure. To secure constant flow of the inert gas, chamber should have gas exhaust connected to the gas bubbler.

To reduce excess heating of the transducers and chamber from the high temperature furnace located in the vacuum/environmental chamber, HT-RUS system should also include cooling subsystem that will allow circulation of the cooling water around transducers and through the chamber walls. Last but not least, will require subsystem for generating, collecting and analyzing ultrasonic signal. The main components of the HT-RUS system are shown in **Figure 3** and the function of each components is described below in more detail.

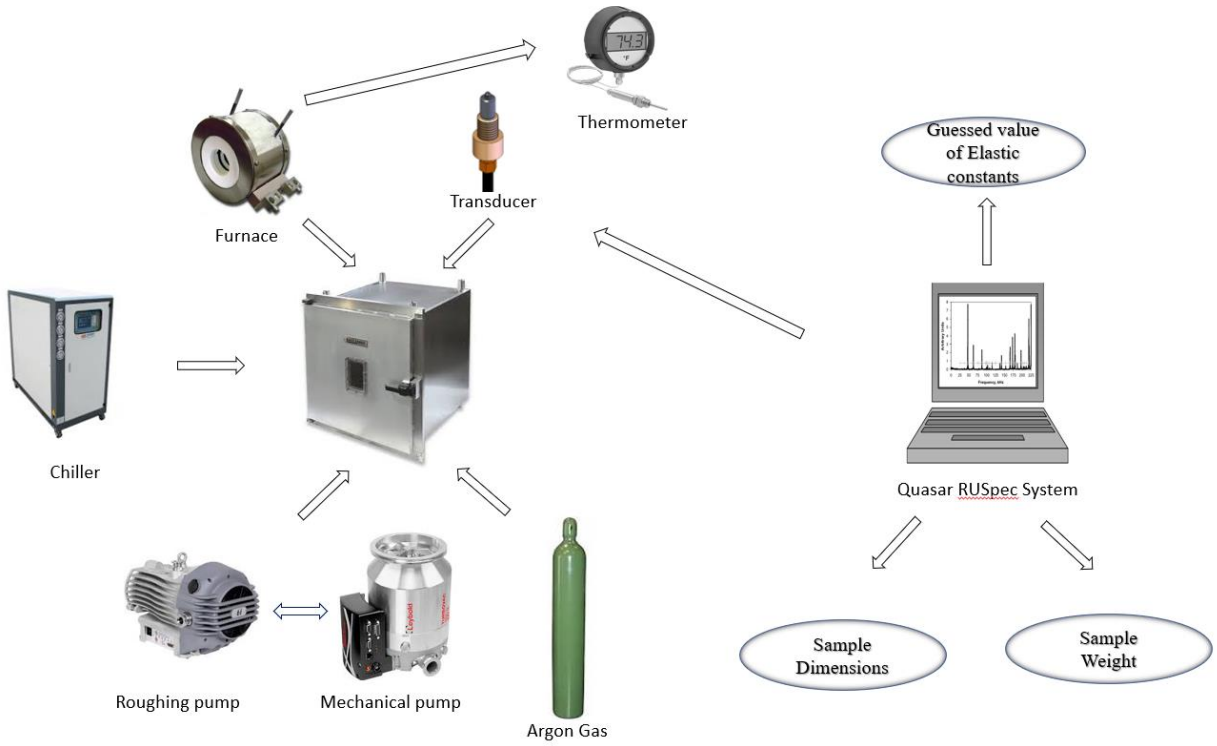

Figure 3. Major components for the designed HT-RUS system

❖ **Stage for tripod measurement setup**

The main function of this stage is kept sample resting on the transducers in the tripod position for RUS measurements, while also allowing easy exchange of the samples and maintenance of extension rods and transducers. Tripod setup is selected for developing high temperature RUS since it allows an easy placement of the sample on transducer as well as use of samples with the larger range of sizes when compared to the tip-to-tip setup. Moreover, there is no stress exerted on the sample during the experiment. The major subcomponents of the stage for tripod setup are described below in more details and presented in **Figure 4**.

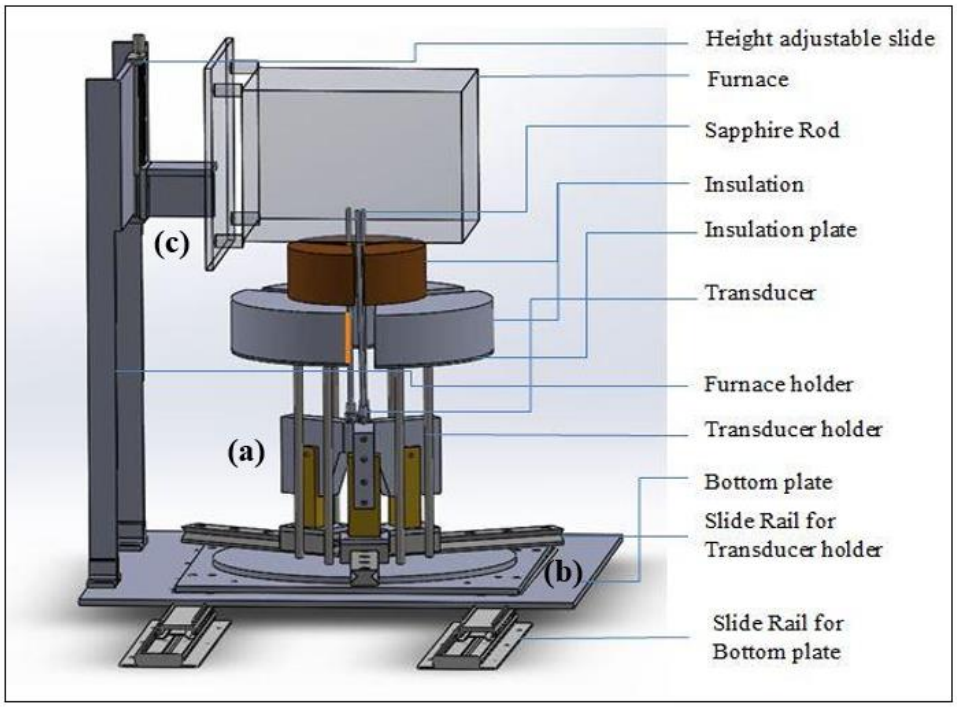

Figure 4. Schematic of major components of the stage for tripod measurement setup in the developed High temperature RUS where (a) is transducer holder, (b) is a bottom plate, and (c) is a furnace holder

Transducers **-** Tripod setup is selected for developing high temperature RUS since it allows an easy placement of the sample on transducer as well as use of samples with the larger range of sizes when compared to the tip-to-tip setup Moreover, there is no stress exerted on the sample during the experiment.

The main functions of three piezoelectric transducers are to generate and transmit to the sample ultrasonic waves at constant amplitude and force sample to vibrate, as well as to detect ultrasonic vibrations of the sample and cover them to the electric signal for further processing. In tripod configuration, one of the transducers generates a resonant signal, the other two transducers detect the signal and converts the mechanical vibrations into electrical signal that is further processed using RUSspec. Transducers contains piezoelectric material, namely zirconate titanate that converts electric signal to mechanical vibrations and vice versa.

Therefore, the major limitation of the transducer is maximum operational temperature piezoelectric zirconate titanate that must be maintain well below their Curie temperatures to obtain a good quality signal around 50°C [28-30].

Extension buffer rods - The main limitation of using RUS at high temperature is the maximum operational temperature of the transducers. Therefore, extension rods have to be attached to the traducers to and from the sample at high temperature, while transducers are kept below ~50 ^{o}C. Three sapphire (Al_2O_3) extension rods will be used as extension rods since sapphire has relatively low thermal conductivity (34-40 W/m·K) and have high stiffness and low attenuation in transmitting the ultrasonic signal. This will allow transmission of the ultrasonic signal between the sample resting on the tips of the extension rods in the furnace and transducers located outside of the furnace which temperature has to be maintained to below ~50 ^{o}C.

Transducer holder - The transducer holder, labeled as (a) in **Figure 4** is designed with four cooling channel to allow for additional cooling of the transducers and maintain their temperature well below ~50 ^{o}C even when the sample in the furnace is heated up to 1600 ^{o}C. A copper is selected as material for transducer holder because of its good heat conductivity when compared to other metals [33]. The cooling channels are built inside the transducer holder **Figure 5,** to maintain the curie temperature of piezoelectric transducers. To provide wide range of sample size for measurement, transducer holder is designed to allow tilting of transducers with attached extension rods about 3° and thus changes of the distance between extension rods tips to accommodate samples of different sizes. Transducer holders are attached to the sliding rail to allow their easily sliding from the central location for replacement of

transducers and/or extension rods. Also, one K-type thermocouple is attached to the transducer holder to monitor its temperature that should not exceed 50 ^{o}C during the high-temperature measurements.

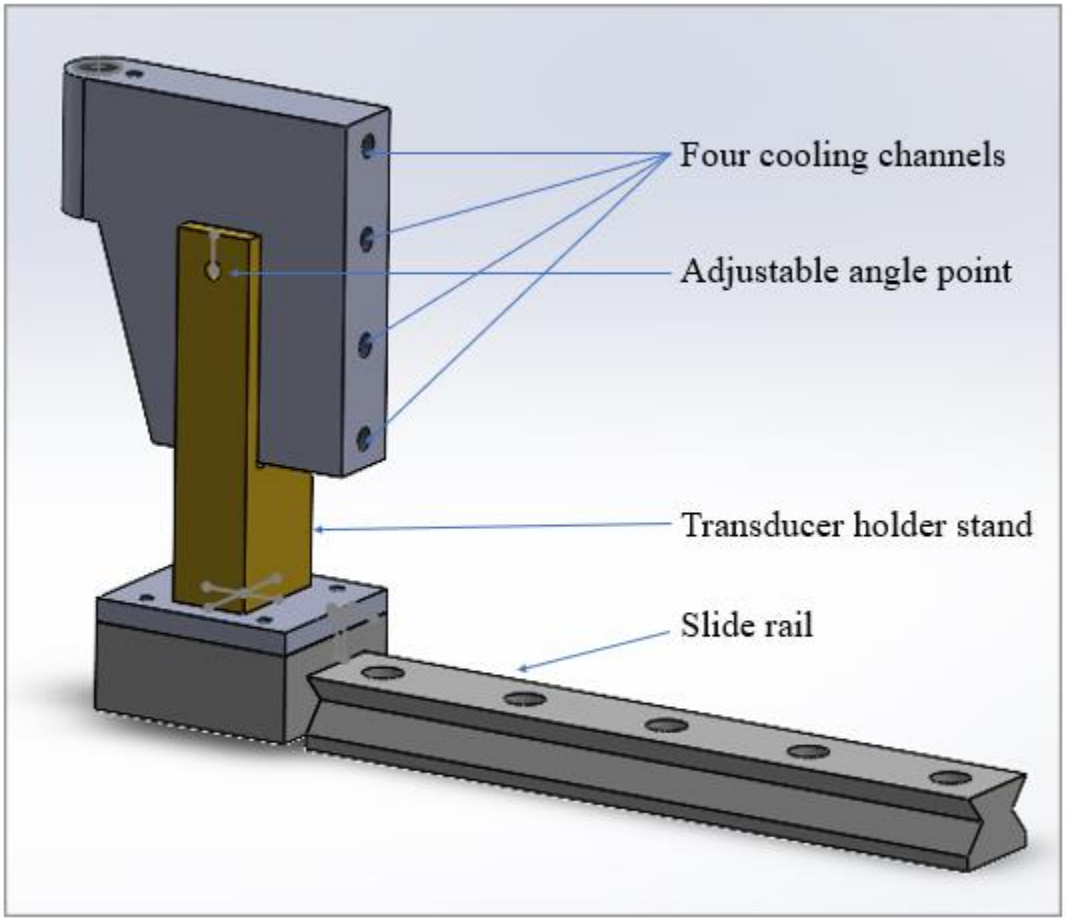

Figure 5. Schematic of the transducer holder with cooling channels

Bottom plate with heat shield - The bottom plate, labeled as (b) in **Figure 4**, is designed to have rectangular plate on the bottom and removable round shaped plate on top. Removable round plate holds three transducer holders on the sliding rails, positioned 180 ^{o} relative, as shown in **Figure 6**. The angle between three transducer holders on the slide rails also enables to test sample with various geometries (discs, cylinders, parallelepipeds) located on top of the three extension rods, and adjust desistance between tips of the extension rods, and adjust

distance between tips of the extension rods to accommodate samples with sizes in range from 15mm to around ~40mm in length. Two slide rails located on the bottom of the bottom plate allows bottom plate with tripod setup and transducers to be slid out of the vacuum/environmental chamber for placing the sample on the top of extension rods and easy maintenance of transducers, furnace, transducer holders and extension rods. Also, the three sets of support rods are placed on top of the bottom plate to hold heat shield plate with the insulation. The heat shield plate has three radial groves for extension rods to pass through them into the furnace located above heat shield plate. Two layers of 2'' thick alumina insulation pads are installed on top of the heat shield plate in order to minimize heat transfer from the furnace to the other components of the measuring stage, especially transducer holders. Bottom plate also holds the furnace holder described in more details below.

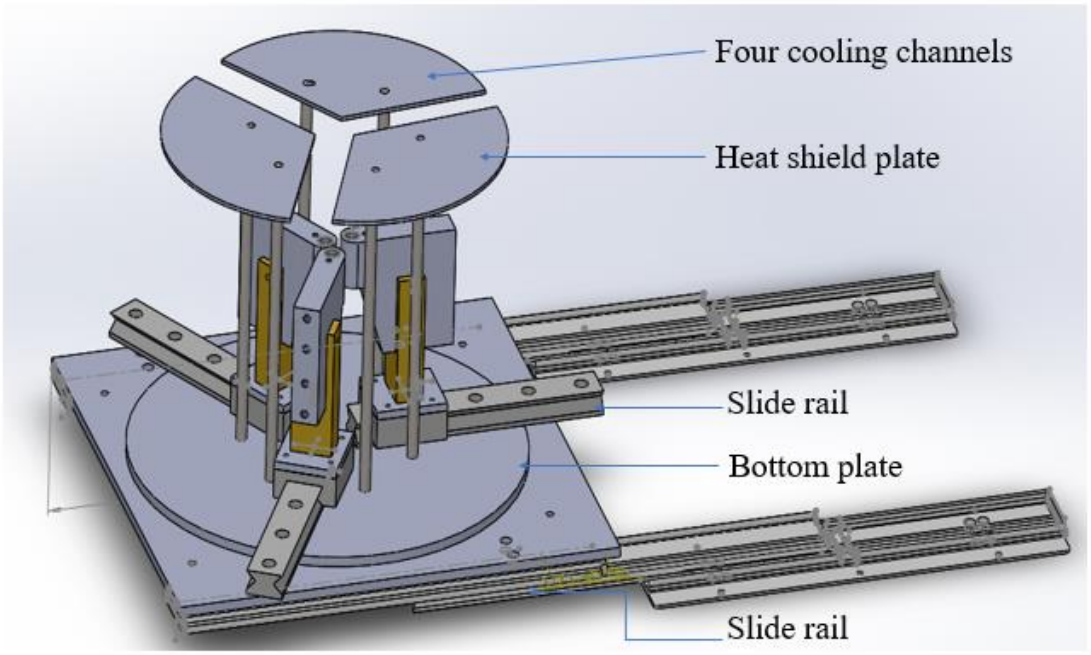

Figure 6. Schematic of the bottom plate with heat shield plate and transducer holders

Height adjustable furnace holder - The main function of furnace holder labeled as (c) in **Figure 4** is to hold the higher temperature furnace housing the tips of the extension rods in the position above the head shield plate. In addition, the furnace holder is designed with knob controlled precision positioning slide to adjust the furnace position in the vertical direction. This allows lifting of the furnace above extension rod tips to place safely the sample on the extension rod tips and lowering it down to touch insulation once the sample is positioned for testing.

- **Furnace**

The main function of the furnace subsystem is provided maximum temperature of 1600°C and it consists of using robust radiator, transformer, and 2 R-type thermocouples controller. The heating zone is designed with inner diameter of 2'' and height of 4" in order to maximize heating inside of the furnace, in addition furnace controller is enabled to control heating rate, power and temperature. Two R-type thermocouple are installed in the furnace. Controlling thermocouple is connected to the furnace controller to monitor temperature in the real time and control heating and cooling rates, while the other one is connected to the overtime reader to monitor and prevent eventual overheating the furnace. High temperature furnace is connected to the transformer and furnace programmable controller that allows heating and cooling the furnace at the controlled rates.

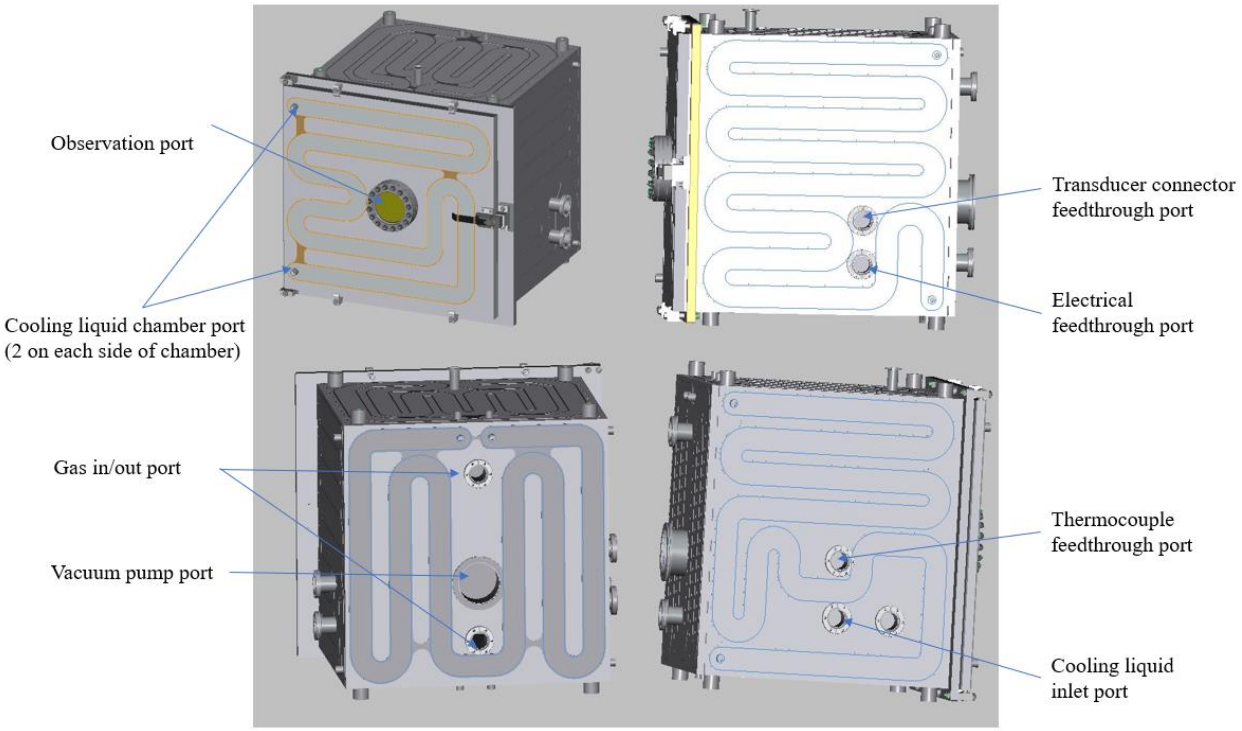

Figure 7. Box chamber assembly with all the ports

❖ **Vacuum/environmental chamber**

To prevent eventual oxidation of sample during testing at elevated temperatures, entire stage for tripod measurement setup with the furnace has to be placed into vacuum/environmental chamber connected to the vacuum pumps and gas supply for testing in ether vacuum, or controlled environment (argon, helium, nitrogen, etc.). This subsystem consists of serval components described in more detail below.

Hydra-cooling Vacuum/environmental chamber – The main function of the vacuum/environmental chamber is provided high vacuum or inert atmosphere for testing of oxidation prone samples at high temperature, **Figure 7**. It encompasses transducer holder with the bottom plate, furnace and furnace holder with K and R type thermocouples. The

vacuum/environmental chamber has to have cooled surfaces to provide additional cooling of the chamber and its interior housing a high temperature furnace. Cooling channels are built on all 6 chamber walls and chamber doors. On the front side of the chamber, an observation point is located for viewing inside of the chamber during measurements and observe any issues with measurement stage or furnace during experimental measurements. On the back side of the chamber, vacuum inlet port is located with gate valve connected to the vacuum pumps, and gas in/out ports with needle valves to control the flow of gases in and out of the furnace. Electrical feedthroughs are located on the right side of the chamber with ceramic insulation insert for safe electric connections whit furnace transformer and controller. Also, single ended transducer connector feedthrough is located in the same side with BNC cable connection in order to connect 3 transducers located in the chamber with RUSpec signal generation and processing unit. On the left side of the chamber, thermocouple feedthroughs are located with four connections: two for K-type and two for R-type thermocouple to enable connections of thermocouples located in the chamber to furnace controller and temperature readers located outside of the chamber. Transducer cooling water inlet and outlet are located on the left wall of the chamber and are designed with swagelok connection in order to connect the hose from chiller to transducer holder to maintain temperature of transducer below 50˚C. Therefore, total of 9 feedthrough ports are designed to meet all the needs to contact components in the vacuum chamber with those located outside of the chamber for the HT-RUS set up, as it is shown **Figure 7**. Vacuum changer is mounted on the top of the custom made stainless steel carts that also have space for furnace transformer below the vacuum chamber.

Vacuum pumps – Two different vacuum pumps are selected: one roughing pump and the other one is turbo pump. Roughing pump has vacuum capability of $10^{-2}\ torr$ and is used to achieve a rough vacuum that is needed before turning on turbo pump which can achieve vacuum of $10^{-4}\ torr$. In addition, pressure gauges are designed to be installed on the vacuum chamber and pump outlet to monitor vacuum pressure at different locations. Vacuum pumps with valves are located on the custom design cart that also supports vacuum pump connection and allows convenient maintenance of vacuum system.

- **Ultrasonic signal generating and processing unit**

A commercially available RUSspec (Magnaflux, Glenview, IL) for generating and processing ultrasonic signal for room temperature RUS has been selected. The unit enables to generate signal within selected frequency range, run tests with at the sweeping frequencies, select frequency steps and dwelling time at each frequency, collect and process signal received from the receiving transducers, and save collected resonant spectra. In addition, also allows analysis of the collected spectra to determine elastic constants for solids with different symmetry (isotropic, cubic, hexagonal, tetragonal, and orthorhombic) and geometry (parallelepiped, cylinder or sphere). This software also determination of ultrasonic attenuation at each resonant peak.

3.3 Description of the developed High-Temperature RUS

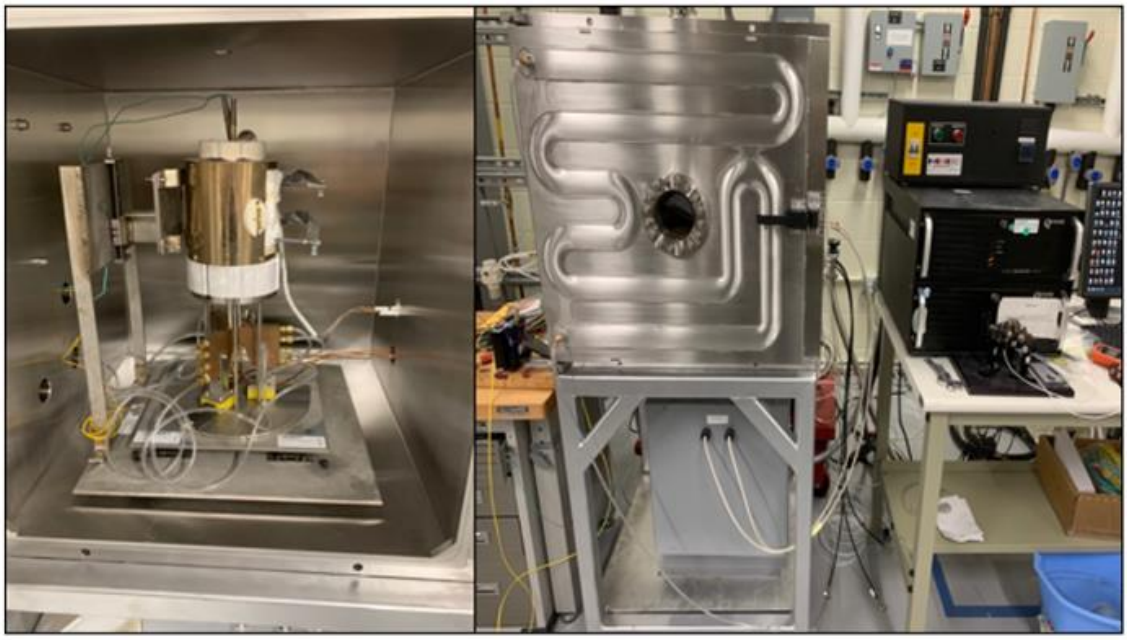

(a) **(b)**

Figure 8. High Temperature RUS system (a) Inside of the chamber (b) Outside of the chamber

HT- RUS system, shown in **Figure 8.a and b** has been developed, designed and built in measure elastic constants of solids from room temperature to elevated temperatures of up to 1600˚C in the controlled environment. The developed system encompasses the commercially available RUS signal generator and software system Quasuar RUSpec (Magnaflux, Glenview, IL) designed for room temperature measurements.

The developed HT- RUS consists of five major subsystems. The first major subsystem of the HT- RUS is transducer stand that holds 3 transducers with attached 6 inches sapphire extension rods, **Figure 9**. In this the tripod configuration, the testing sample sits on the tips of the 3 extension rods located in the furnace, and ultrasonic waves with sweeping frequencies are transmitted to form one transducer through extension rods to the sample, while vibrations of the samples were

transited back through extension rods to two receiving transducers where they are converted in into electric signal. The most important limiting factor for design of the transducer stand. It must hold piezoelectric transducers in place and allow their cooling to below 50˚C, even when the temperature at the tip of extension rods is 1600^{o}C. This is crucial because modified commercial available transducers (Magnaflux, Glenview, IL) used for developed HT-RUS encompasses zirconate titanate or barium titanate piezoelectric material that are operational only to temperatures up to 50˚C. To achieve good cooling of the transducers, four cooling channels were designed for each transducer holder to allow circulation of the cooling water and cool down the transducer holder under the limiting temperature. The coolant channeled holder is pre-assembled with four Swagelok pipe fittings connected with polyurethane tubing. Also, transducer holders are placed on the linear sliders for easy adjustment of the spacing between transducers roads to accommodate samples with different sizes and to allow for easy replacement of all components **Figure 9.a**.

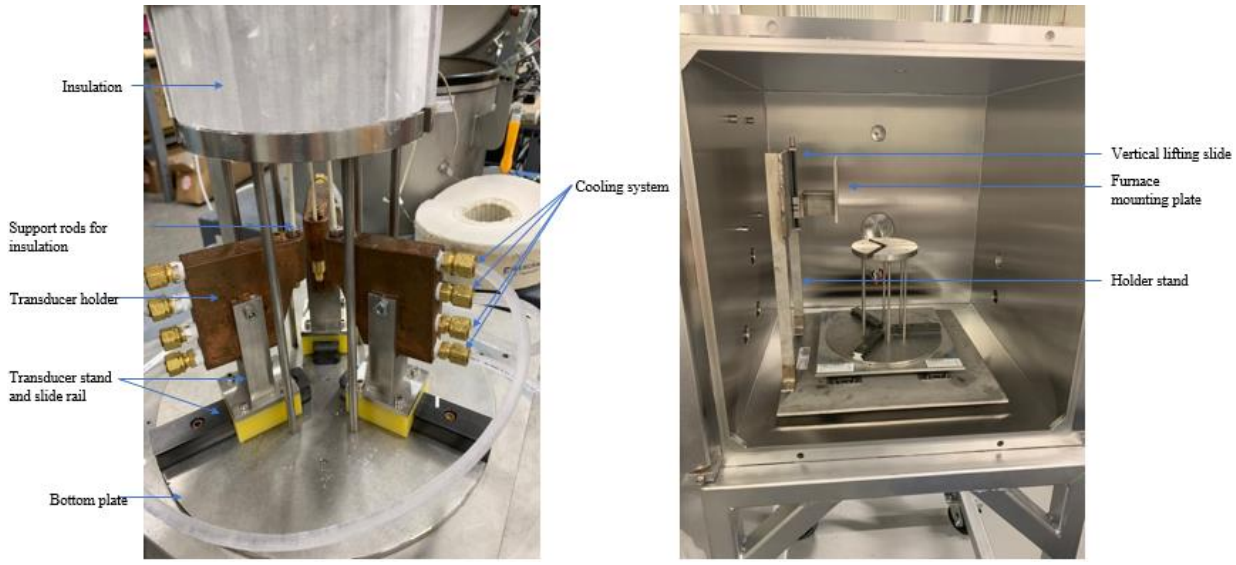

Figure 9. (a) Stage for tripod measurement setup with the furnace, (b) Bottom plate with furnace holder and heat shield located in the vacuum chamber

The second subsystem of this setup is the base plate, **Figure 9.b**. Base plate holds transducer stands and the heat shield placed between transducer holder and the furnace. It is design to allow easy access to the transducer setup for their replacement when it is placed in the vacuum chamber. More importantly, this design contains sliders which enable the plate with the transducer holder to be conveniently moved outside of the vacuum chamber from repair and maintenance, especially for the replacement of transducers and extension rods. Furthermore, additional insulation plates are placed in the thermal shield holder for reducing heat radiation and conduction from the heat source (furnace) **Figure 8.a** to the transducers.

The third subsystem of proposed design is the furnace holder with the furnace, furnace controller and insulations. Furnace holder consists of a base plate and a set of 10-inch long stainless-steel stands and supports (Micropyretics Heaters International) heater with maximum temperature of 1600 ^{o}C. Since transducer must be kept under 50 ^{o}C while experiment takes place at up to 1600 ^{o}C, two layers of alumina insulating pads are installed under the furnace to minimize heat radiation and conduction coming from the furnace **Figure 9.b**. The furnace holder is design to allow easy lifting up of the furnace to place a testing sample on the tips of the extension rods and lower it down to close after sample is put in place.

(a) **(b)**

Figure 10. Chamber frame with a vacuum/environmental chamber (a) front view (b) bottom view

To reduce the heat radiation around the furnace inside of the chamber, a liquid cooling system is designed on all 6 sides of the chamber **Figure 10.a and b**. On the front side of the chamber, an observation point is located for viewing inside of the chamber. On the back side of the chamber, Vacuum inlet ports and gas in/out ports are designed. On the right side of the chamber, an electrical feedthrough and single ended transducer connector feedthrough is located. On the left side of the chamber, thermocouple feedthrough as well as cooling liquid inlet and outlet are located. There is a total of 9 ports designed to meet all the connections for the HT-RUS set up.

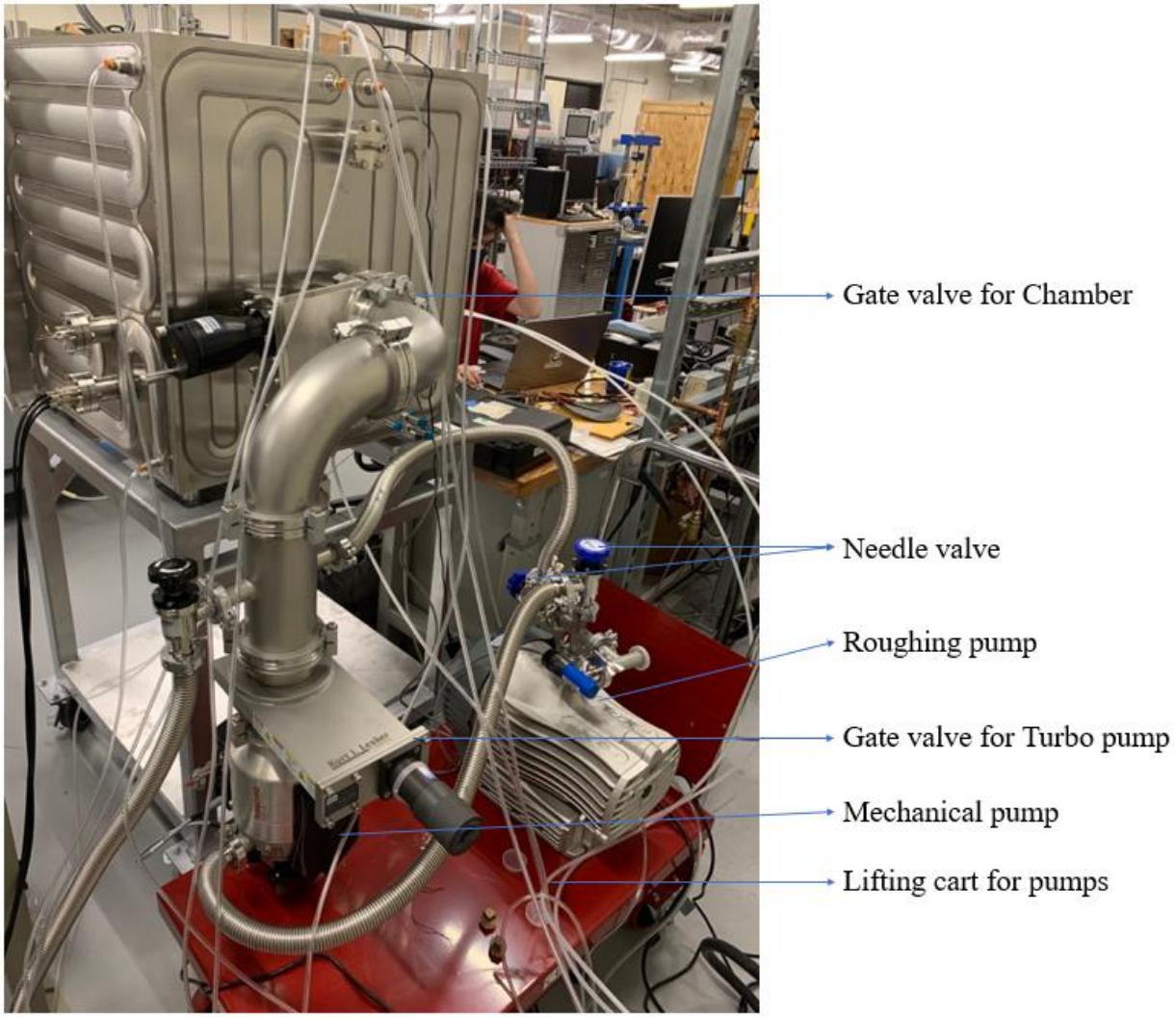

Figure 11. Vacuum pump connection for HT-RUS

A vacuum pump system is also custom designed and built that consist of a lifting cart, two gate valves and two on/off needle valves to control vacuum flows to the chamber, **Figure 11**. The procedure of vacuum pump system are described in more details the HT-RUS Manual in **Appendix B**. Lastly, Chamber frame is specially built to locate the chamber on top of the frame. The mount table is capable of carrying 2000 lbs, load, including vacuum/environmental chamber with bottom plate, transducer holders and furnace subsystem in it, and furnace transformer under

the frame. Also, since there are spaces needed for bottom of the chamber to install cooling water line for hydra-cooling system, opening in the middle of the frame is designed **Figure 10**.

The fifth subsystem is a RUSpec which is generator and analyzer. Newly developed HT-RUS system utilizes a commercially available RUS software Quasar RUSpec (Magnaflux, Glenview, IL) to calculate elastic moduli of the solid by utilizing an inverse, iterative algorithm for solving equation of minimizing Lagragian, **Figure 12.** This system requires initial values for elastic constants referred to as "guessed" elastic constants which can be obtained from *ab initio* calculation, or other sources [31]. Typically, first 20-50 resonant frequencies are used to compute the elastic constants and by inputting dimensions and mass of the sample, usually in the shape of parallelepiped disc or cylinder. It is crucial to measure the dimensions at a precision of down to 2 microns. The fitting-program is based on the previously discussed multidimensional algorithm (see Section 2.3) which starting from the set of initial or "guessed" values for the elastic constants, compares measured resonant frequencies for the first 20-50 resonant peaks and calculated resonant frequencies iteratively until minimum root-mean-square (RMS) error is achieved (usually less than 0.4%). In the case of isotropic material, only two "guessed" elastic constants C_{11} and C_{44} are required **Figure 13** as a initial "guessed" values, while for the system with lowers symmetry, larger number of the initial constants in needed depending on the symmetry of the system, to initiate iterative process of determining elastic constants form the measured resonant frequencies using RUSpec software.

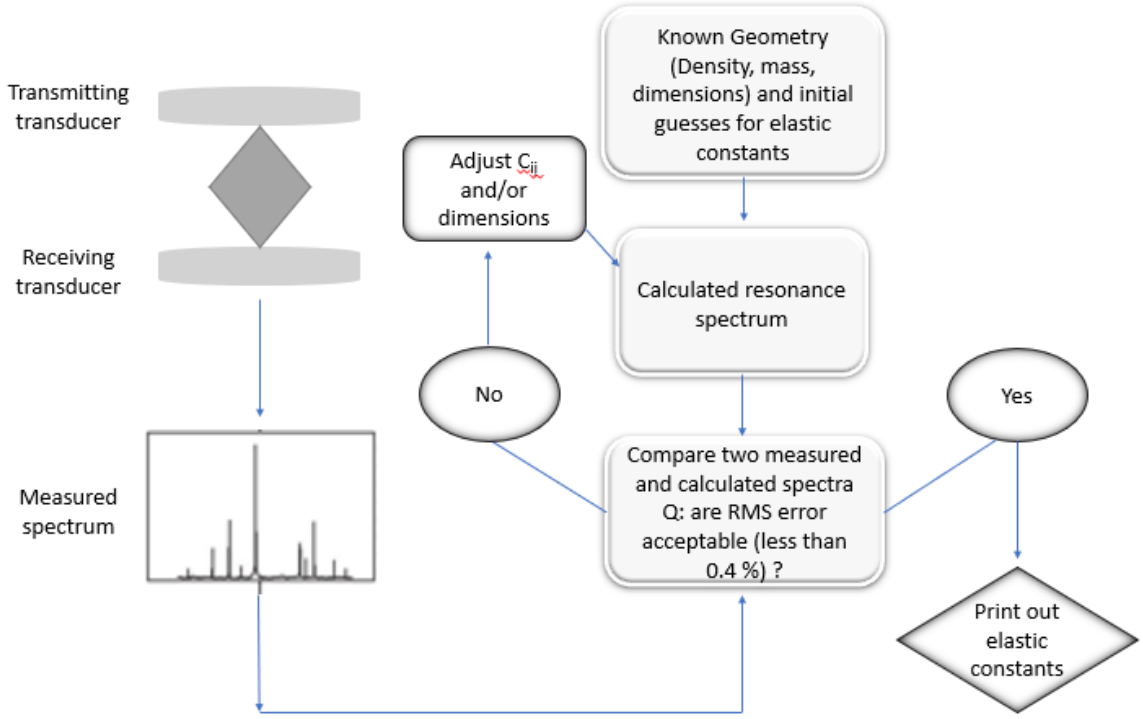

Figure 12. Multidimensional algorithm of the RUS system [12]

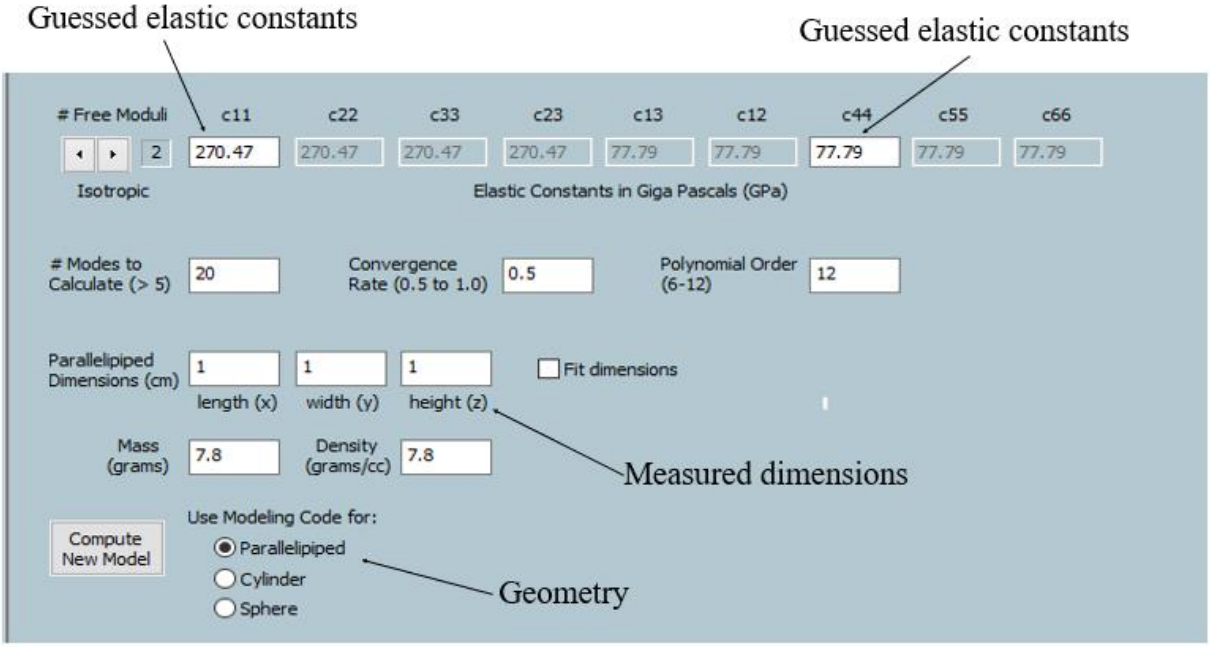

Figure 13. Screen shot of RUSpec

3.4 Specifications of the instrument to build

The major components of developed HT-RUS with their detailed specification are described in **Table 1** including the manufacturer of the components and their abilities.

Table 1. Specification of the Newly developed HT-RUS component

#	Component	Specification
1	Furnace	Manufacturer: MHI-Inc Model: Roburst Radiator Max.Temp: 1600˚C Heating element: Molybdenum Disilicide Max Power: 1425Watts Heated length: 4inch, Overall length: 6’’, ID: 2’’, OD: 6’’ Location: 750 Redna Terrace Cincinnati OH 45215
2	Vacuum chamber	Manufacturer: Kurt J, Lesker Model: Hydra-cooling chamber Chamber size: 24’’ x 24’’ x 24’’ Cooling channel: 6 sides Material: 304L Stainless steel Location: 1925 Route 51 Jefferson Hills, PA 15025
3	RUS software	Manufacturer: Magnaflux Quasar Software: RUSpec Frequency range: 0 to 3000 Khz Location: 155 Harlem Avenue Glenview, IL 60025
4	Vacuum pump (Roughing)	Manufacturer: Edward Model: nXDS 6i Max pressure: $2\ x10^{-2} torr$ Location: 1845 S. Lewis St. , Anaheim, CA 92805
5	Vacuum pump (Mechanical)	Manufacturer: Leybold-Inc Model: TURBOVAC 350i(X) Max pressure: $5\ x\ 10^{-5}\ torr$ Permissible fore vacuum pressure: 5 x $10^{-1}\ torr$ Location: 6005 Enterprise Drive PA 15632

Table 1. Continued

#	Component	Specification
6	Transducer	Manufacturer: Magnaflux Model: Standard transducer Assembly-less tip Material: Brass Location: 155 Harlem Avenue Glenview, IL 6002
7	Buffer Rod	Manufacturer: Kyocera Material: Sapphire Dimension: OD: .125'', Height: 6'', round tip only one side Location: 740E Campbell Rd # 320 Richardson TX 75081
8	Insulation	Manufacturer: Kyocera Material: Alumina Type Al-28/1800 Max temp: 1800˚C Location: 740E Campbell Rd # 320 Richardson TX 75081
9	Transducer holder with cooling channel	Material of Transducer holder: Brass Material of cooling hose: Polyethylene Maximum operating temp: 50˚C
10	Position slide	Manufacturer: Mcmaster-carr Maximum load capacity: 490 lbs Max carriage: 46mm Location: 1901 Riverside Pkwy. Douglasville, GA 30135
11	Slide rail	Manufacturer: Mcmaster-carr Max load capacity: 150lb Max carriage: 20inch Location: 1901 Riverside Pkwy. Douglasville, GA 30135
12	Chiller	Manufacturer: Texas A&M central cooling system Temperature range: -25˚C to 150˚C Flow rate: 5Liter per min

3.5 Experimental procedure

As described above, RUS system is very sensitive to geometry and symmetry of the sample, in which the preparation requires a quite precise process. Thus, samples, such as rectangular parallelepiped and cylinder, must be well polished. If opposite faces are not parallel, the resonant

frequencies of the sample will be significantly affected. This leads to a weak relationship between measured and calculated frequencies with root-mean-square (RMS) values larger than 0.4%. In such conditions, the values derived from the elastic moduli are usually considered to be unreliable. A well-prepared sample then, is held on top of the three 6-inch extension rods with 1mm in diameter and rounded tips where samples are glued to the transducer using a low viscosity Loctite® 406 Instant Adhesive, **Figure 14**. Low viscosity glue enables the application of a very thin layer of adhesive between buffer rods and transducers, thus ensuring a successful transition of ultrasonic waves. The entire setup can be placed in a custom designed hydra-cooling vacuum chamber in controlled atmosphere. RUS software and furnace heater then can be operated to measure a full set of elastic constants at a desired temperature.

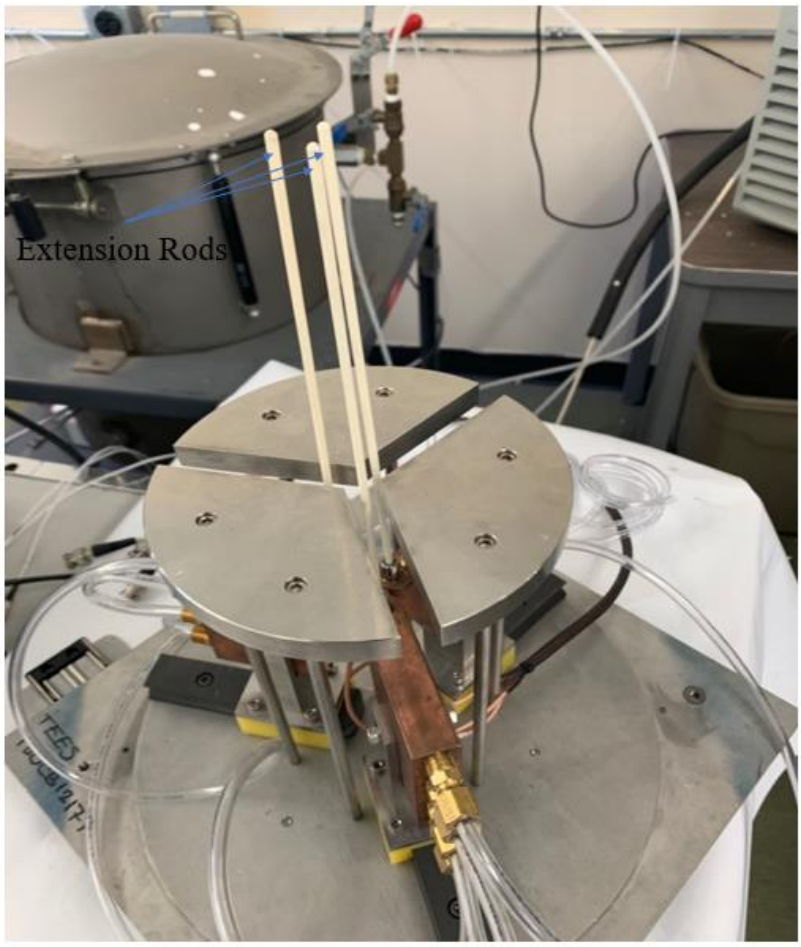

Figure 14. Newly developed HT-RUS tripod setup with transducer holder .

4. TESTING OF THE DEVELOPED HT-RUS APPARATUS

After assembly of the HT-RUS system, individual subsystems were first tested for proper operation before measuring elastic constants of some selected materials, and the results of those tests are described below. In addition, resonant spectra of several different materials, namely Alumina, Silicon-Nitride, Tantalum Carbide were collected.

4.1 Vacuum system testing

A roughing pump and a turbo pump were first tested to ensure that they can achieve proper vacuum levels. High vacuum grease was applied to all vacuum connections to prevent any leaks. The vacuum/environmental chamber was evacuated first until vacuum of roughly to 10^{-1} torr was reached. After that, turbo pump was turned on left running for 60 minutes until stable vacuums of 6.0 x 10^{-4} *torr* and 9.5 x 10^{-3} *torr*, we reached at the turbo pump and chamber, respectively as shown in **Figure 15**. This drop in the vacuum level between vacuum pump and chamber is expected for ledge volume vacuum chamber with a lot of walkthrough connections. In addition, to check for any additional, alcohol was sprayed around all sealed openings, and not pressure changes of bubbling was observed.

After vacuum testing, the vacuum/environmental chamber was backfilled to with ultra-high purity (UHP) Ar to the pressure slightly above atmospheric pressure, i.e. until gas bubbles formed in the bubbler installed on the gas exhaust line on the chamber. Once again, all sealed openings were checked on eventual leak by spraying soap water around all openings, and no formation of bubbles was noticed.

Figure 15. Vacuum gauge of pressure inside the chamber

4.2 Culling water circulation system

To check for eventual leaks in the cooling water circulations channels in both transducer holders and chamber walls, cooling water at the rate of 5L/m has been circulated for 2hours. No liking has been observed.

4.2 Infrared (IR) testing of HT-RUS setup

Since transducers has to be cooled below maximum of 50 $^{\circ}$C at all the time, temperature distribution on the transducers, extension rods and surface of the furnace was monitored using IR camera, while heating the furnace. Without a running cooling water through the cooling channels in the transducer holder, the heat transfer from the furnace, primarily through extension rods resulted in the heating of the transducers to temperature of more than of 50 $^{\circ}$C, when the temperature in the furnace reached only ~ 800 $^{\circ}$C. However, when running the cooling water through transducer holders at a temperature 5 $^{\circ}$C and at a rate of 5 L/min. The temperature of the transducers was well below 50 ^{o}C even after reaching 1600 ^{o}C in the furnace, as shown in the infrared images in **Figure 16**. Also, **Figure 16** shows that the temperature in the zone below the furnace is around 68 $^{\circ}$C when furnace is heated up to 1600 ^{o}C, indicating that the furnace is well insulated, heat transfer through the opening for extension rods at the bottom of the furnace is minimal.

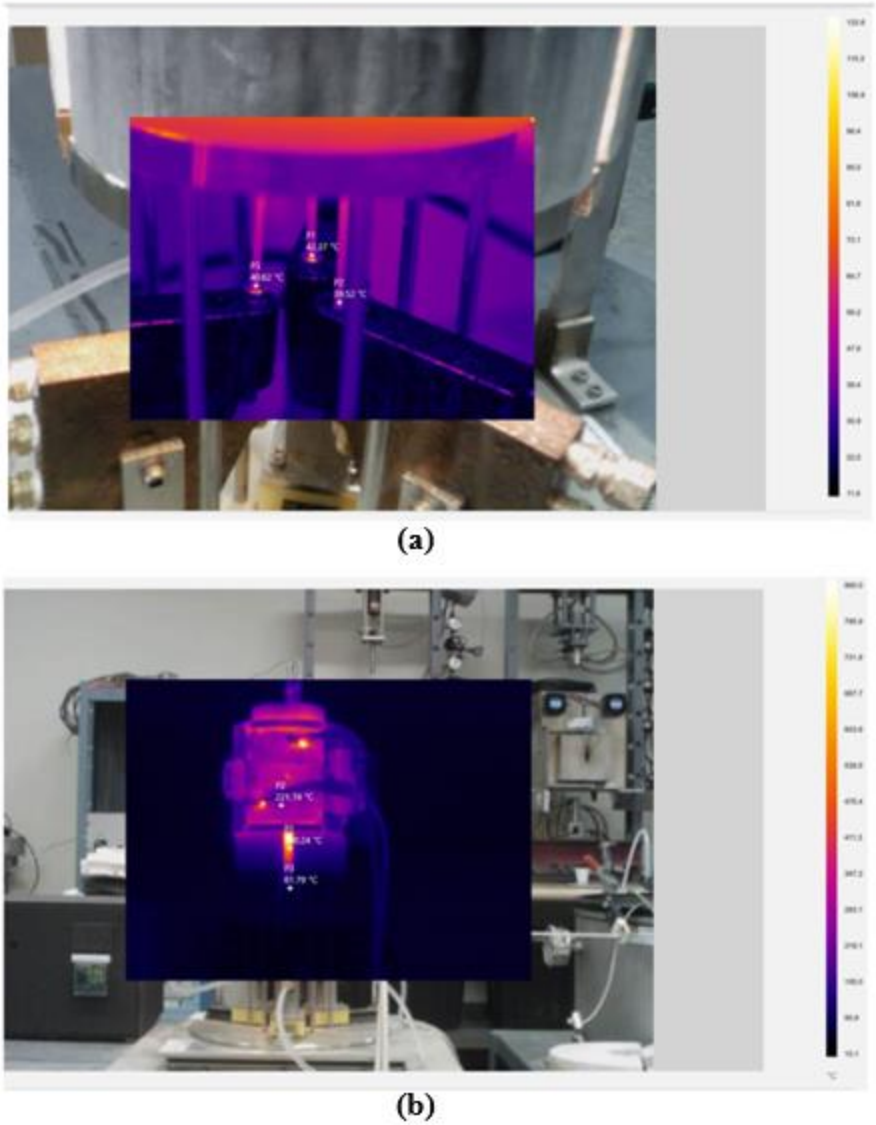

Figure 16. Infrared images of the temperature distribution during heating HT-RUS furnace at 1600 ºC (a) Transducer temperature (b) Furnace temperature

4.3 Comparison of resonant spectra collected using HT-RUS and commercial apparatus at room temperature.

The resonant spectra collected using HT-RUS setup were compared to those collected using commercially available tripod RUS setup (Magnaflux, Glenview, IL) at room temperature, to check for the accuracy in resonant frequencies detected using developed HT-RUS. All resonant spectra were collected using the same Alumina (Al_2O_3) discs 31.77 mm in diameter and 3.84 mm thick. **Figure 17** shows resonant spectra for alumina sample collected using HT-RUS and commercial apparatuses, while **Table 2** summarizes passion of the resonant peaks detected from those resonant spectra.

In general, due to the dissipation of signal appearing within the sapphire extension rods of developed setup, resonant peaks in the spectra collected using HT-RUS apparatus show a lower overall intensity when compared to that collected using commercial setup, **Figure 17**. However, more importantly, the resonant frequencies collected at room temperature using developed HT-RUS setup in 20-500 kHz range are almost identical to those collected using commercial apparatus, and the difference between resonant frequencies determined using those two setups is always lower than 0.01%.

In addition, Young's, shear and bulk moduli, as well as Poisson's ratio of the alumina sample was determined using RUSpec software from resonant spectra collected using developed HT-RUS and commercially available set up. Results summarized in **Table 3** show an excellent agreement between elastic moduli determined using two different RUS setups, with the maximum error of 0.01% for shear modulus.

.

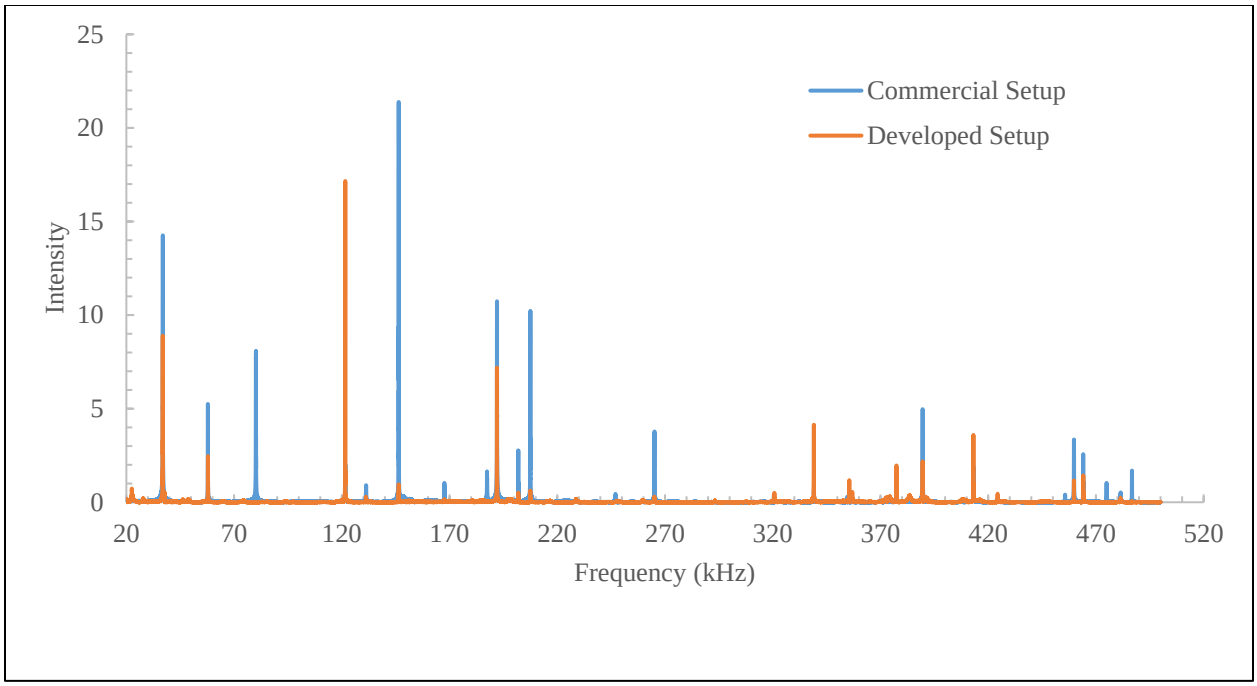

Figure 17. Resonant spectra of Al_2O_3 collected using developed HT-RUS and commercial setups at room temperature

Table 2. Comparisons of frequencies of resonant peaks collected at room temperature using developed HT-RUS and commercial setup.

	Developed HT-RUS	Commercial RUS	
Mode	Resonant peak (kHz)	Resonant peak (kHz)	% error
1	36.844	36.847	-0.0081
2	36.844	36.847	-0.0081
3	57.802	57.808	-0.0104
4	80.099	80.106	-0.0087
5	80.099	80.106	-0.0087
6	121.531	121.543	-0.0099
7	121.31	121.543	-0.1917
8	131.159	131.17	-0.0084
9	131.16	131.171	-0.0084
10	146.411	146.423	-0.0082
11	146.411	146.423	-0.0082
12	167.641	167.656	-0.0089
13	167.641	167.656	-0.0089
14	187.435	187.451	-0.0085
15	187.435	187.451	-0.0085
16	191.954	191.973	-0.0099
17	191.954	191.973	-0.0099
18	202.025	202.047	-0.0109
19	207.483	207.503	-0.0096
20	224.358	224.376	-0.0080

	Developed HT-RUS	Commercial RUS	
Mode	Resonant peak (kHz)	Resonant peak (kHz)	% error
21	224.358	224.376	-0.0080
22	247.111	247.132	-0.0085
23	247.113	247.134	-0.0085
24	259.54	259.563	-0.0089
25	259.54	259.563	-0.0089
26	265.072	265.097	-0.0094
27	265.072	265.097	-0.0094
28	291.638	291.662	-0.0082
29	291.638	291.662	-0.0082
30	293.185	293.213	-0.0095
31	293.185	293.213	-0.0095
32	308.984	309.01	-0.0084
33	308.984	309.01	-0.0084
34	320.779	320.804	-0.0078
35	339.135	339.166	-0.0091
36	339.145	339.176	-0.0091
37	354.622	354.651	-0.0082
38	354.622	354.651	-0.0082
39	355.675	355.71	-0.0098
40	355.675	355.71	-0.0098

Table 3. Room temperature elastic moduli and Possion's ratio of Al_2O_3 determined from resonant spectra collected using developed HT-RUS and commercial setup

Al_2O_3	Young's Modulus (GPa)	Shear Modulus (GPa)	Bulk modulus (GPa)	Poisson ratio	RMS error(%)
Commercial setup	373.148	151.34	232.764	0.233	0.057
Developed setup	373.094	151.34	232.569	0.233	0.081

4.4 Elastic moduli of Aluminum Oxide determined using developed HT-RUS

Aluminum oxide (Al_2O_3) was first chosen for testing at elevated temperatures using newly developed HT-RUS setup due to its good stability at high temperatures and almost liner decrease of elastic moduli with temperature. In this study, a sample in the shape of discs with diameter of 31.77 mm, thickness of 3.84 mm and the density of 3.89g/cm^3 was used to determine elastic moduli from resonant spectra.

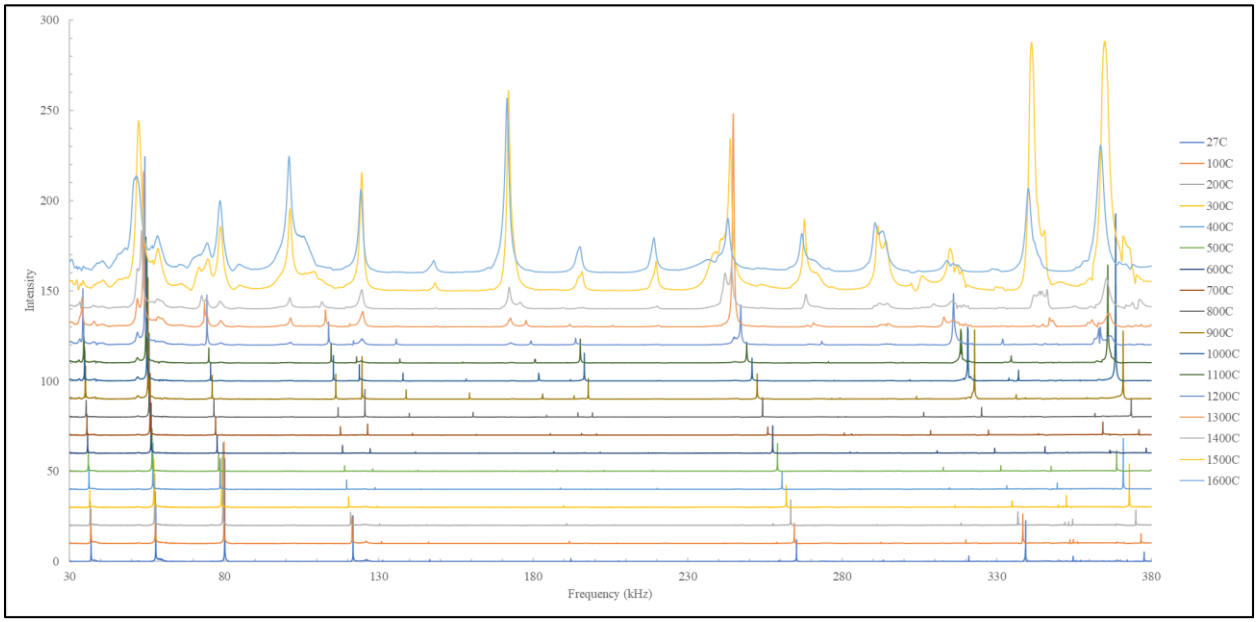

Figure 18. Resonant spectra of Al_2O_3 at different temperature

Resonant spectra were collected using developed HT-RUS starting form room temperature (25 ^oC) to 1600 ^oC, in temperature increments of 100 ^oC during heating and cooling. **Figure 18** shows resonant spectra collected during heating for alumna sample, while **Figure 19** shows Young's and Shear moduli determined using RUSpec software from collected resonant spectra collected during heating to 1600 ^oC and cooling back to the room temperature. **Figure 18** shows that resonant peak positions shift toward lower frequencies with increasing due to decrease in elastic moduli. As shown in **Figure 19**, both Young's and shear moduli decrease almost linearly

with increasing temperature. The values of elastic moduli determined during heating and cooling are in excellent agreement and varies for less than approximately 0.2% at any temperature in 25 °C - 1600 °C temperature range.

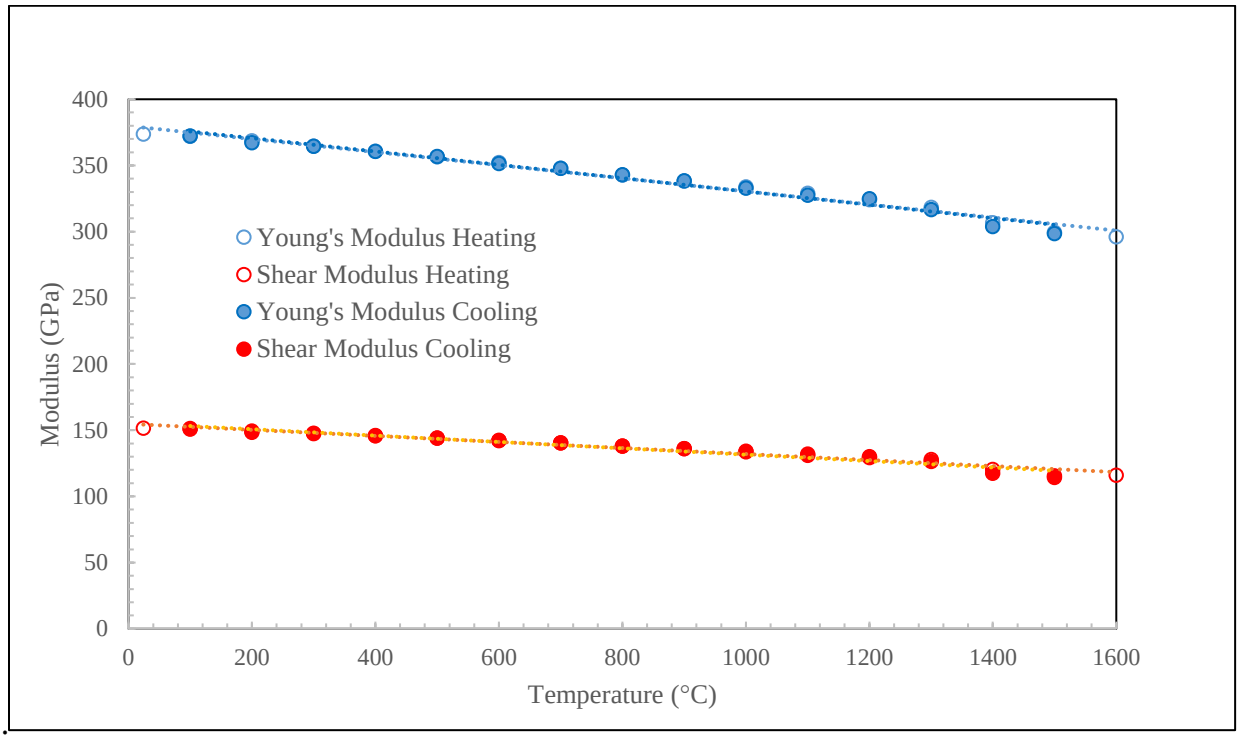

Figure 19. Young's and Shear modulus of Al_2O_3 sample determined using developed HT-RUS

Changes of Young's and shear moduli determined for Al_2O_3 sample using developed RUS are compared in **Figure 20** to those of Al_2O_3 published by Goto and Anderson [34] and Watchtman and Lam[35] determined using RUS and impulse excitation technique, respectively. While decrease in elastic moduli with increasing temperature determined in this study shows quite similar trends to data published in the literature (**Figure 20**) [34-35,37], the value obtained in this study are lower than value reported by Goto and Anderson [34], but higher than those reported by Watchtman and Lam [35] at any given temperature. The reason for this discrepancy lies in the

different density of the samples used to obtain results summarized in **Figure 20**; while sample used in this study had density of 3.89g/cm^3, sample used by Goto and Anderson was much denser with density of 3.982 g/cm^3, while that used Wachtman and Lam was less dense with density of 3.710 g/cm^3. Therefore, it is reasonable to conclude that differences in measured moduli can be related to different residual porosities of the sintered polycrystalline alumina samples used for testing in different studies [37]. Therefore, when elastic moduli at any temperature from **Figure 19** where normalized to the room temperatures values, and plotted vs. temperature in **Figure 20**, it can be observed that decrease in elastic moduli with increasing temperature obtained herein using developed HT-RUS are in good agreement with those reported by Goto and Anderson [35] and Watchtman and Lam [36].

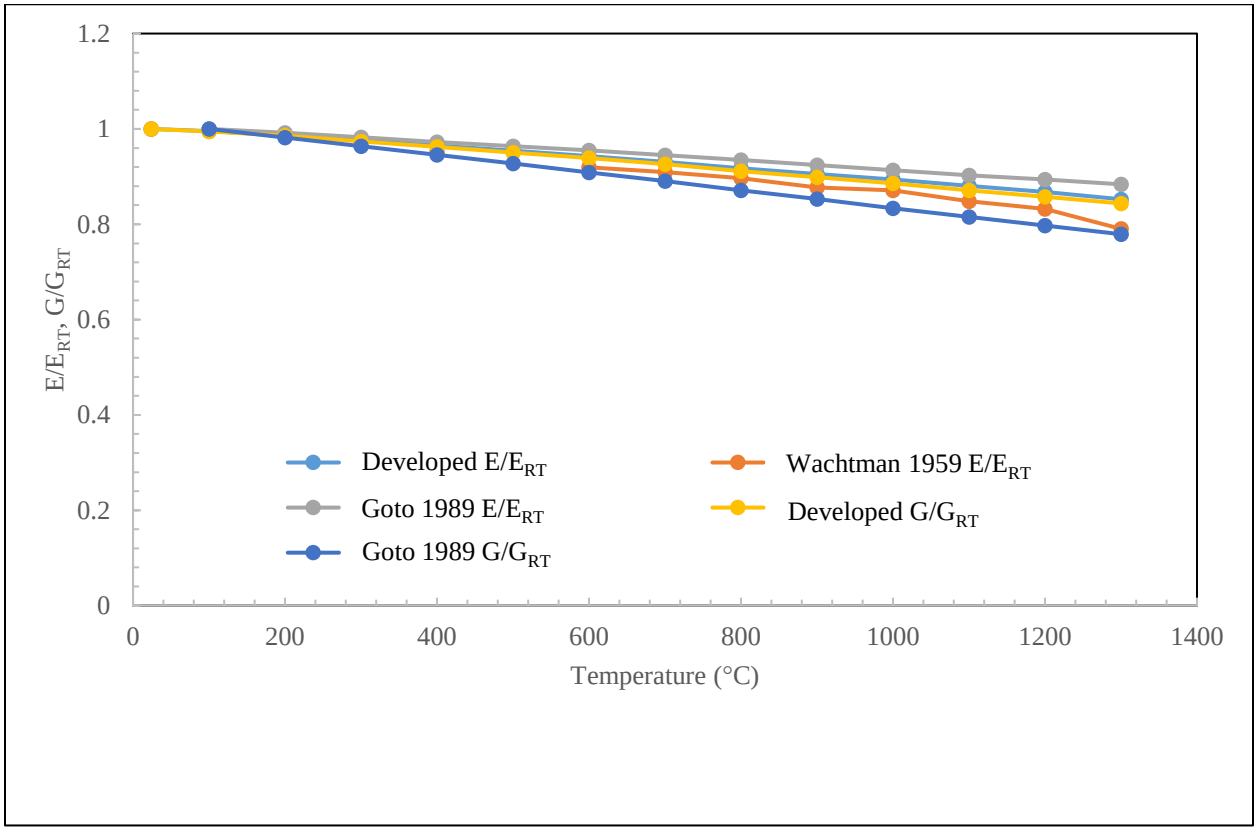

Figure 20. Comparison of normalized Young's and shear modulus of Al_2O_3 at different temperatures, obtained using developed HT-RUS and reported Goto and Anderson [34] and Watchtman and Lam [35]

As a result, newly developed HT-RUS has not only an excellent capability of measuring a full set of elastic constants in broad range of temperatures up to 1600 $^{\circ}$C, but also provides results for that are in good agreement with previously published results in the literature.

4.5 Silicon Nitride

Polycrystalline **s**ilicon nitride (*Si_3N_4)* is valued engineering ceramic for many because it has low density and good thermal stability but high strength, toughness, and exceptionally high thermal shock resistance when compared to other monolithic ceramic materials. It also shows very small decrease in elastic moduli with increasing temperature [38]. In this study, Silicon Nitride (*Si_3N_4*) sample in the shape of discs with diameter of 20.02 mm, thickness of 2.05 mm 3.22 g/cm^3 was also tested using newly developed HT-RUS apparatus. **Figure 21** shows resonant spectra in 30-215 kHZ range collected from room temperature to 1500 ^oC, in increments of 100 ^oC. The result in **Figure 21** clearly shows that resonant peaks are shifting slightly towards lower frequencies with increasing temperatures below 1100 ^oC, due to decrease in elastic moduli. However, at 1100 ^oC and above, a significant broadening of the resonant peaks can be observed that is typical manifestation of increased ultrasonic attenuation in the material. This attenuation can be attributed to the softening of the glassy phase that is commonly present in the sintered polycrystalline *Si_3N_4* samples. Due to significant broadening of the peaks at and above 1100 ^oC, those resonant spectra cannot be deconvoluted to determine elastic moduli using commercially available RUSpec software with acceptable level of RMS error.

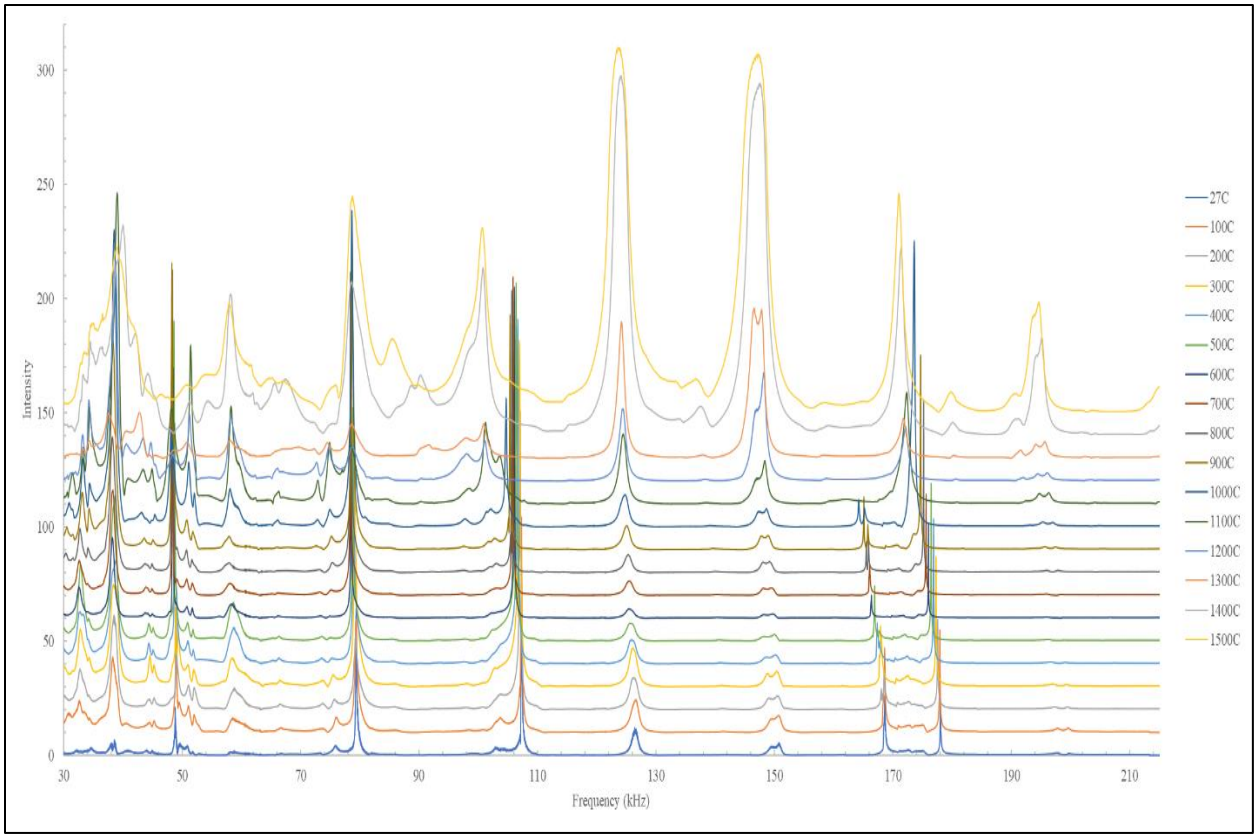

Figure 21. Resonant spectra of Si_3N_4 at different temperature

However, the resonant spectra of Si_3N_4 up to 1000 ^oC can be deconvoluted using RUSpec software to determine Young's and shear moduli at various temperatures, and results are summarized in **Figure 22**. According to **Figure 22**, both Young's modulus and Shear modulus decrease monotonically with increasing temperature, showing decrease of only approximately 4% at 1000 $^{\circ}C$ when compared to the values obtained at room temperature.

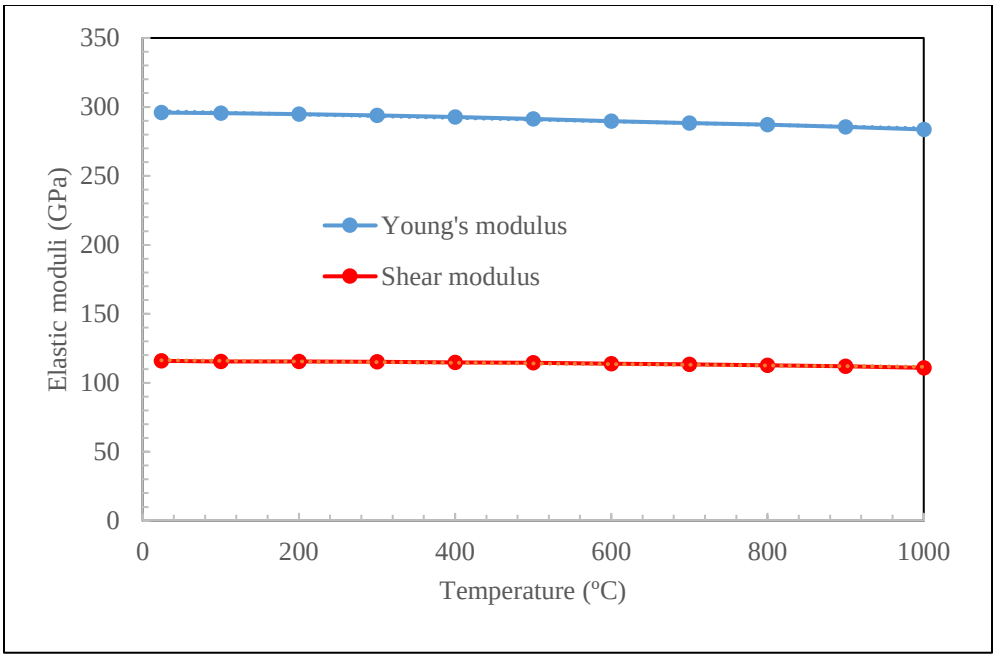

Figure 22. Young's and Shear moduli of Si_3N_4 determined using developed HT-RUS

W.A. Fate [39] determined Young modulus Si_3N_4 in 25-1000 °C using impulse excitation technique, and their results are compared to the results obtained using developed HT-RUS in **Figure 23**. As in the case of Si_3N_4 samples used in this study, it had density of 3.22 g/cm^3, while sample used by W.A. Fate [39] had much lower density of 2.7 g/cm^3. Due to relatively higher density of the sample used for testing in the developed HT-RUS, the Young's modulus obtained in this study are higher than that published by W.A. Fate [39]. However, changes of the Young's modus with temperature obtained by both methods follow the similar trends as shown in **Figure 23**.

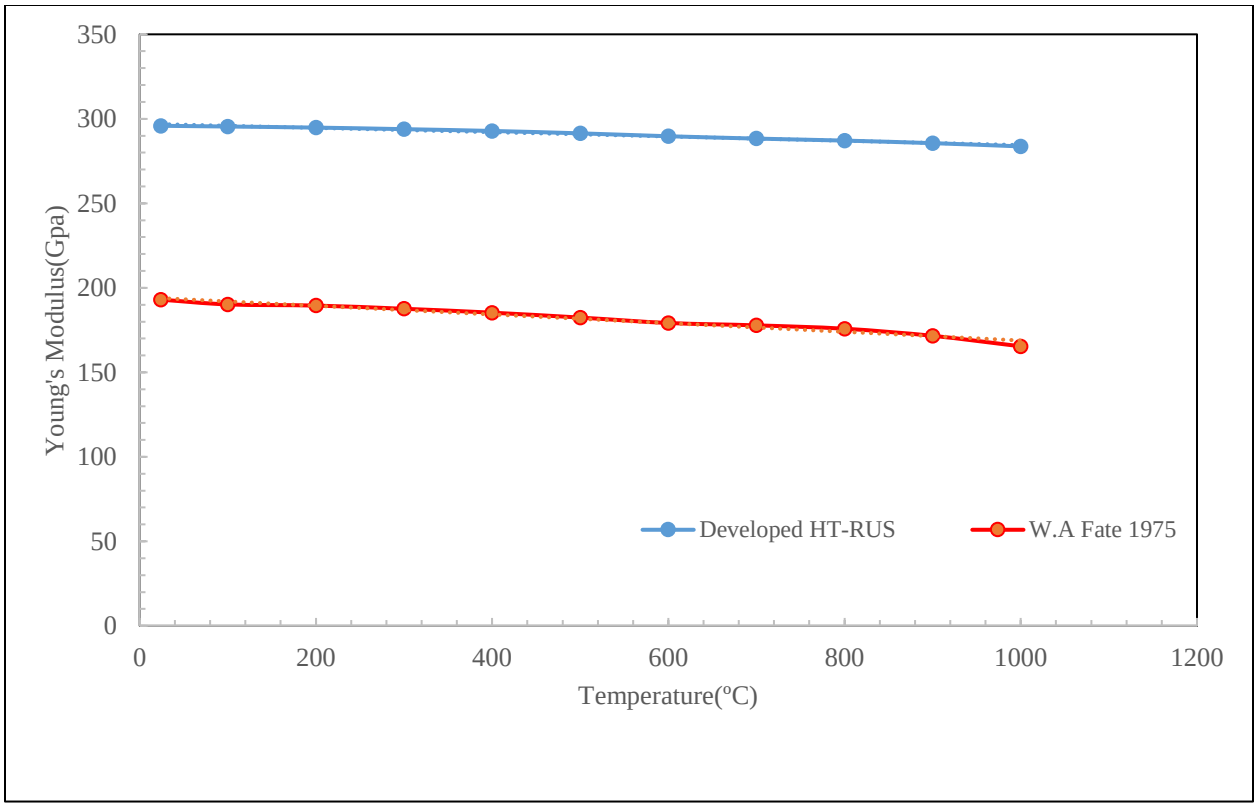

Figure 23. Young's modulus of Si_3N_4 comparison with literature value [39]

4.6 Tantalum Carbide

Tantalum Carbide, (ζ-Ta_4C_{3-x}) is a new ceramic material with promising application at ultra-high temperatures for aircraft and rockets in aerospace industries. ζ-Ta_4C_{3-x} is a one of the unique phases in TaC binary carbide system with rhombohedral crystal structure and has received attractive attention in recent studies due to their high melting point of 3768 ^oC, high oxidation resistance, and high fracture toughness [40-42].

To determine elastic properties of this newly developed ceramic, ζ-Ta_4C_{3-x} was tested by using developed HT-RUS apparatus using disc-shaped sample with diameter of 20.02 mm thickness of 2.02 mm in thickness and density of 14.506 g/cm^3, and collected resonant spectra up to 1200^{o}C are shown in **Figure 24**. Once again, resonant peaks shift towards lower frequencies with increasing temperature, due to decrease in elastic constants.

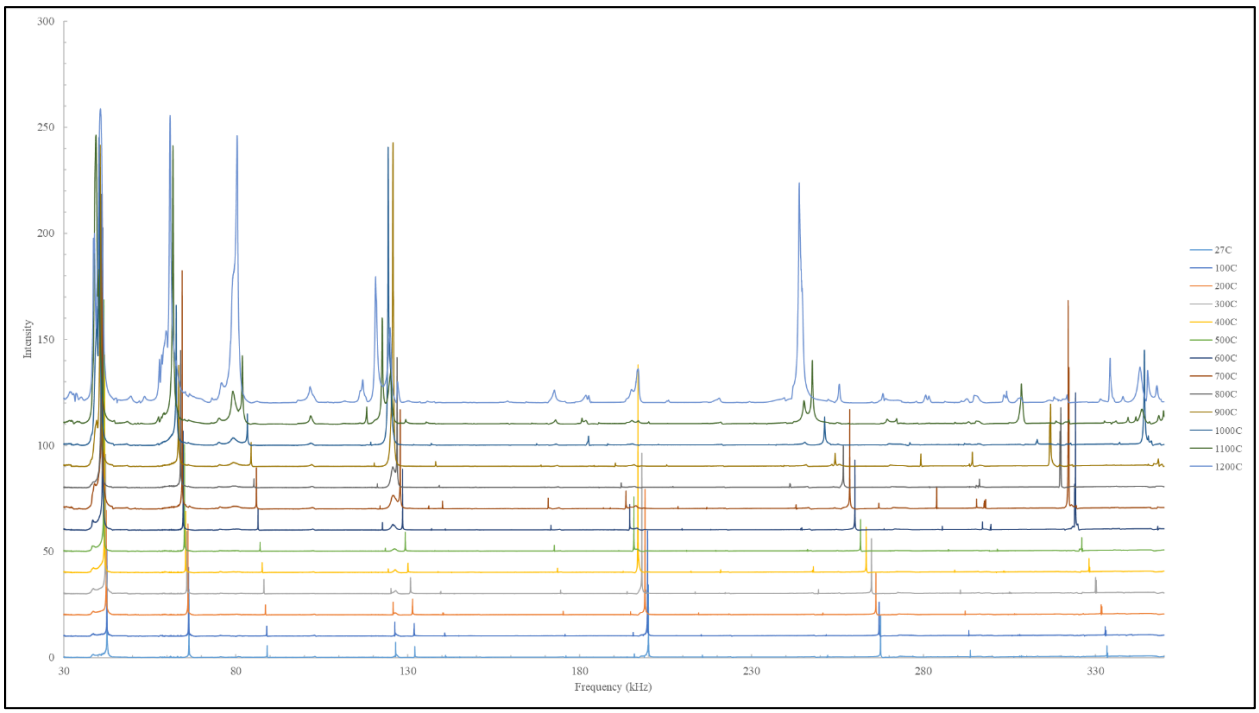

Figure 24. Resonant spectra of ζ-Ta_4C_{3-x} at different temperature

The Young's and Shear moduli at room temperature determined using developed HT-RUS are compared to the results preciously published in the literature in **Table 4**. The results in **Table 4** show that theoretical values of elastic moduli reported using impulse excitation method by Evan C. Schwind [40] is considerably lower than these measured in this study using developed HT-RUS due to their varying density of the samples. As in the case of ζ-Ta_4C_{3-x} samples used in this study had density of 14.506 g/cm^3, while sample used by Evan C. Schwind [40] was much less dense with density of 14.3 g/cm^3. Typically, the variation in the magnitude of the elastic constants can be due to the varying density of the samples used in different experiments as the porosity of the samples has an important influence on the elastic properties of ceramics [36].

Table 4. A full set of elastic constant of ζ-Ta_4C_{3-x} at room temperature [40]

ζ-Ta_4C_{3-x}	Young's Modulus (GPa)	Shear Modulus (GPa)	Bulk modulus (GPa)	Poisson ratio	Density g/cm^3
Developed HT-RUS	415.069	166.84	270.131	0.244	14.506
Evan C. Schwind	379	150	267	0.322	14.3

Furthermore ζ-Ta_4C_{3-x} was tested with using newly developed HT-RUS at the temperature range of room temperature up to 1200°C. As shown in **Figure 25**, both Young's and Shear moduli drop monotonically for up to 16% in 25-1200°C temperature range.

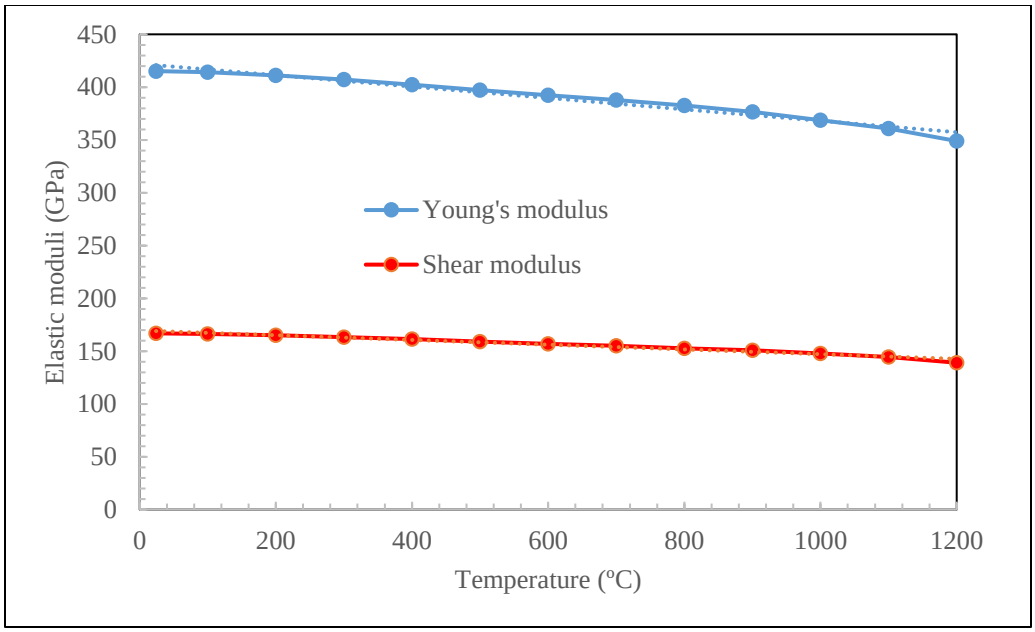

Figure 25. Young's and shear moduli of ζ-Ta_4C_{3-x} as a function of temperature between room temperature and 1200 ºC

5. CONCLUSION AND FUTURE WORK

In this research, a unique custom-made apparatus for high temperature Resonant Ultrasonic Spectroscopy allowing determination of the full set of elastic constants the materials from room temperature to 1600 ^{o}C in vacuum or controlled environment was design, developed, built and tested. This apparatus utilizes transmission of the ultrasonic waves through sapphire extension rods from/to cooled transducer/receiver to/from the sample kept at elevated temperatures. This, designed instrument allows testing samples at very high temperatures while keeping transducers below their maximum operating temperature of 50 ^{o}C. The measurement set up is located in the vacuum/environmental chamber with a custom-designed hydra cooling channels in the chamber walls to provide additional cooling of the chamber housing high temperature furnace. Developed High temperature RUS apparatus was used to measure a full set of elastic constants of solids at temperatures ranging from room temperature up to 1600 $^{\circ}$C in a controlled environment for several materials and compare those results with data available in the literature, and results are summarized as following:

1. Aluminum oxide (Al_2O_3) was tested using newly developed a HT-RUS tripod setup up to 1600°C. The resonant spectra collected at room temperature match those collected using commercially available room temperature RUS system, and the elastic moduli determined using those two setups are different for less than 0.01%. More importantly, the Young's and Shear moduli determined using developed HT-RUS shows declining trend with increasing temperature up to maximum testing temperature of 1600^{o}C that is in good

agreement with the results obtained using other measurement techniques and published in the open literature.

2. Polycrystalline Silicon Nitride (Si_3N_4) was also chosen for measuring Young's and shear moduli using newly developed HT-RUS up to 1000 ^{o}C. The comparison of result demonstrated that both moduli decrease monotonically with temperature, up to approximately 96% of their values at room temperature value once the testing temperature reached 1000^{o}C. Because of the high ultrasonic attenuation in Si_3N_4, resonate spectra collected above 1000^{o}C, could not have been deconvoluted to determine elastic moduli. Nevertheless, the results obtained up to 1000 ^{o}C are in good agreement with previously published results collected using different measurement techniques.

3. Elastic moduli of the newly developed high temperature material, namely ζ-Tantalum Carbide, (ζ-Ta_4C_{3-x}) were studied with newly developed HT-RUS up to 1200°C. It was found that both Yong's modulus and Shear modulus decreased approximately 16% with increasing temperature in a linear fashion. Most importantly, comparison of room temperature elastic moduli obtained using developed HT-RUS and data reported in the literature between once again show good agreement for both Young's and shear modulus.

In summary, newly developed HT-RUS proves to be an accurate and very powerful apparatus for measuring a full set of elastic constants in broad range of temperatures up to 1600 $^{\circ}$C in controlled environments, using only one small sample. This system will be useful for understanding elastic properties and anelastic relaxation processes for different materials. The capability of proposed development will not only allow fast and convenient characterization of

various materials but also enhance research in material science, engineering, physics, and chemistry.

To continue developing different types of RUS systems, the following tasks must be considered.

1. develop a system capable of measuring elastic constants in liquid helium with temperature ranges of 4K to 800K under a magnetic field up to 8T;
2. develop Tip-to-Tip setup with utilizing only two transducers to measure smaller specimens at the high temperatures.
3. develop setup for measuring under electric filed for characterizing electroactive materials, such as piezoelectric or electrostrictive materials.

REFERENCE

1. Grossmann, J., et al., *Highly sensitive simple homodyne phase detector for ultrasonic pulse-echo measurements.* Review of Scientific Instruments, 2016. **87**(4): p. 044901.
2. Bartels, A. and D. Harder, *Non-invasive determination of systolic blood pressure by heart sound pattern analysis.* Clinical Physics and Physiological Measurement, 1992. **13**(3): p. 249-256.
3. Renken, M.C., et al. *Accuracy of resonant ultrasound spectroscopy: an experimental study*. in *1997 IEEE Ultrasonics Symposium Proceedings. An International Symposium (Cat. No.97CH36118)*. 1997.
4. Migliory, A. and J. Sarrao, *Resonant ultrasound spectroscopy: applications to physics, material measurements and non-destructive evaluation.* Wiley, New York, 1997. **1**: p. 17-22.
5. Fraser, D. and R. LeCraw, *Novel method of measuring elastic and anelastic properties of solids.* Review of Scientific Instruments, 1964. **35**(9): p. 1113-1115.
6. Anderson, O.L., et al., *Elastic properties of a micro-breccia, igneous rock and lunar fines from Apollo 11 mission.* Geochimica et Cosmochimica Acta Supplement, 1970. **1**: p. 1959.
7. Demarest Jr, H.H., *Cube-resonance method to determine the elastic constants of solids.* The Journal of the Acoustical Society of America, 1971. **49**(3B): p. 768-775.
8. Sumino, Y., et al., *Measurement of elastic constants and internal frictions on single-crystal MgO by rectangular parallelepiped resonance.* Journal of Physics of the Earth, 1976. **24**(3): p. 263-273.

9. Ohno, I., *Temperature variation of elasticity of α-quartz by the rectangular parallelepiped resonance method.* The Journal of the Acoustical Society of America, 1996. **99**(4): p. 2579-2603.

10. Migliori, A. and T.W. Darling, *Resonant ultrasound spectroscopy for materials studies and non-destructive testing.* Ultrasonics, 1996. **34**(2-5): p. 473-476.

11. Kinney, J., et al., *Resonant ultrasound spectroscopy measurements of the elastic constants of human dentin.* Journal of biomechanics, 2004. **37**(4): p. 437-441.

12. Li, G. and J.R. Gladden, *High Temperature Resonant Ultrasound Spectroscopy: A Review.* International Journal of Spectroscopy, 2010. **2010**: p. 206362.

13. Leisure, R.G. and F.A. Willis, *Resonant ultrasound spectroscopy.* Journal of Physics: Condensed Matter, 1997. **9**(28): p. 6001-6029.

14. Migliori, A. and J.D. Maynard, *Implementation of a modern resonant ultrasound spectroscopy system for the measurement of the elastic moduli of small solid specimens (7 pages)*. 2005, AMERICAN INSTITUTE OF PHYSICS: United States. p. 121301.

15. Dowling, N.E., *Mechanical behavior of materials : engineering methods for deformation, fracture, and fatigue. 4th ed. Norman E. Dowling*. 4th ed. ed. 2013: Pearson.

16. Shull, P.J., *Nondestructive evaluation : theory, techniques, and applications. edited by Peter J. Shull*. Mechanical engineering: 142. 2002: Marcel Dekker.

17. Flynn, K. and M. Radovic, *Evaluation of defects in materials using resonant ultrasound spectroscopy*. 2011, Springer Science + Business Media: Great Britain. p. 2548.

18. Markham, M., *Measurement of elastic constants by the ultrasonic pulse method.* British Journal of Applied Physics, 1957. **8**(S6): p. S56.

19. Radovic, M., E. Lara-Curzio, and L. Riester, *Comparison of different experimental techniques for determination of elastic properties of solids.* Materials Science and Engineering: A, 2004. **368**(1): p. 56-70.

20. Schwarz, R. and J. Vuorinen, *Resonant ultrasound spectroscopy: applications, current status and limitations.* Journal of Alloys and Compounds, 2000. **310**(1-2): p. 243-250.

21. Ohno, I., *Free vibration of a rectangular parallelepiped crystal and its application to determination of elastic constants of orthorhombic crystals.* Journal of Physics of the Earth, 1976. **24**(4): p. 355-379.

22. Ohno, I., et al., *Determination of elastic constants of trigonal crystals by the rectangular parallelepiped resonance method.* Journal of Physics and Chemistry of Solids, 1986. **47**(12): p. 1103-1108.

23. Davis, E.S., et al., *Resonant Ultrasound Spectroscopy studies of Berea sandstone at high temperature.* Journal of Geophysical Research: Solid Earth, 2016. **121**(9): p. 6401-6410.

24. Davulis, P., et al. *High temperature elastic constants of langatate from RUS measurements up to 1100° C*. in *2008 IEEE Ultrasonics Symposium*. 2008. IEEE.

25. Radovic, M., et al., *On the elastic properties and mechanical damping of Ti3SiC2, Ti3GeC2, Ti3Si0.5Al0.5C2 and Ti_2AlC in the 300–1573K temperature range.* Acta Materialia, 2006. **54**(10): p. 2757-2767.

26. Gudlur, P., et al., *Thermal and mechanical properties of Al/Al_2O_3 composites at elevated temperatures.* Materials Science and Engineering: A, 2012. **531**: p. 18-27.

27. Anderson, O.L., *Rectangular parallelepiped resonance—A technique of resonance ultrasound and its applications to the determination of elasticity at high temperatures.* The Journal of the Acoustical Society of America, 1992. **91**(4): p. 2245-2253.

28. Zhang, S., et al., *Piezoelectric materials for high power, high temperature applications.* Materials Letters, 2005. **59**(27): p. 3471-3475.

29. Tressler, J.F., S. Alkoy, and R.E. Newnham, *Piezoelectric Sensors and Sensor Materials.* Journal of Electroceramics, 1998. **2**(4): p. 257-272.

30. Wolf, R.A. and S. Trolier-McKinstry, *Temperature dependence of the piezoelectric response in lead zirconate titanate films.* Journal of Applied Physics, 2004. **95**(3): p. 1397-1406.

31. Migliori, A., et al., *Resonant ultrasound spectroscopic techniques for measurement of the elastic moduli of solids.* Physica B: Condensed Matter, 1993. **183**(1-2): p. 1-24.

32. Spoor, P.S., *Elastic Properties of Novel Materials Using PVDF Film and Resonance Ultrasound Spectroscopy*. 1997, PENNSYLVANIA STATE UNIV UNIVERSITY PARK DEPT OF PHYSICS.

33. Berman, R., *Heat conductivity of non-metallic crystals.* Contemporary Physics, 1973. **14**(2): p. 101-117.

34. Goto, T., et al., *Elastic constants of corundum up to 1825 K.* Journal of Geophysical Research: Solid Earth, 1989. **94**(B6): p. 7588-7602.

35. Wachtman JR., J.B. and D.G. Lam JR., *Young's Modulus of Various Refractory Materials as a Function of Temperature.* Journal of the American Ceramic Society, 1959. **42**(5): p. 254-260.

36. Fan, X.F., et al., *Room temperature elastic properties of gadolinia-doped ceria as a function of porosity.* Ceramics International, 2013. **39**(6): p. 6877-6886.

37. Hardy, D. and D.J. Green, *Mechanical properties of a partially sintered alumina.* Journal of the European Ceramic Society, 1995. **15**(8): p. 769-775.

38. Bocanegra-Bernal, M.H. and B. Matovic, *Mechanical properties of silicon nitride-based ceramics and its use in structural applications at high temperatures.* Materials Science and Engineering: A, 2010. **527**(6): p. 1314-1338.

39. Fate, W.A., *High-temperature elastic moduli of polycrystalline silicon nitride.* Journal of Applied Physics, 1975. **46**(6): p. 2375-2377.

40. Schwind, E.C., G.E. Hilmas, and W.G. Fahrenholtz, *Thermal properties and elastic constants of ζ-Ta4C3−x.* Journal of the American Ceramic Society, 2020. **103**(5): p. 2986-2990.

41. Sygnatowicz, M., R.A. Cutler, and D.K. Shetty, *zeta-Ta4C3-x: A High Fracture Toughness Carbide with Rising-Crack-Growth-Resistance (R-Curve) Behavior.* Journal of the Amertican Ceramic Seociety, 2015. **98**(8): p. 2601-2608.

42. Sygnatowicz, M., et al., *Processing of Dense ζ- Ta4 C3− x by Reaction Sintering of Ta and TaC Powder Mixture.* Journal of the American Ceramic Society, 2014. **97**(12): p. 3826-3834.

APPENDIX A

Technical drawings

1. Hydra-cooling chamber (Kurt J. Lesker)

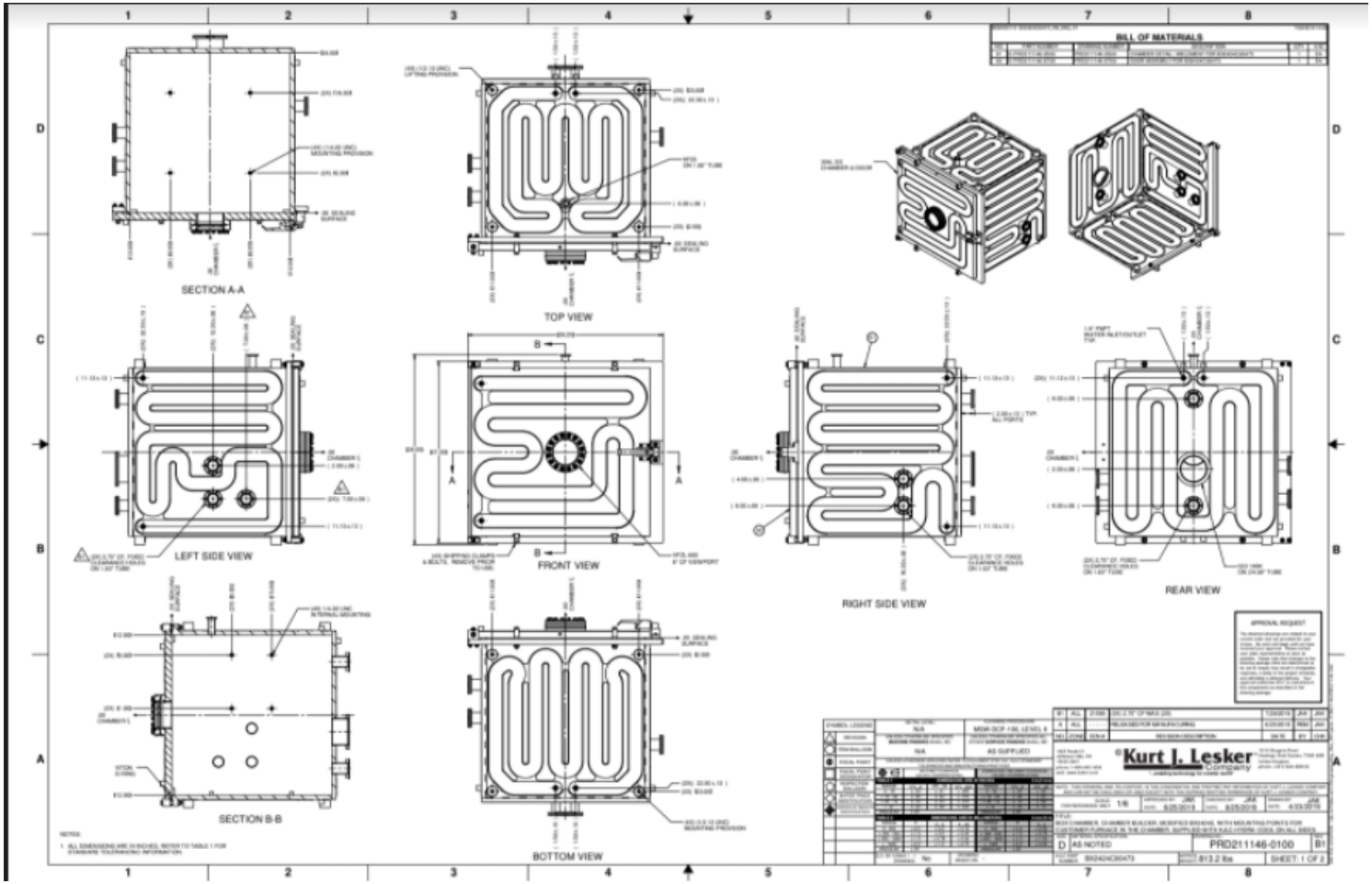

2. Transducer (Magnaflux)

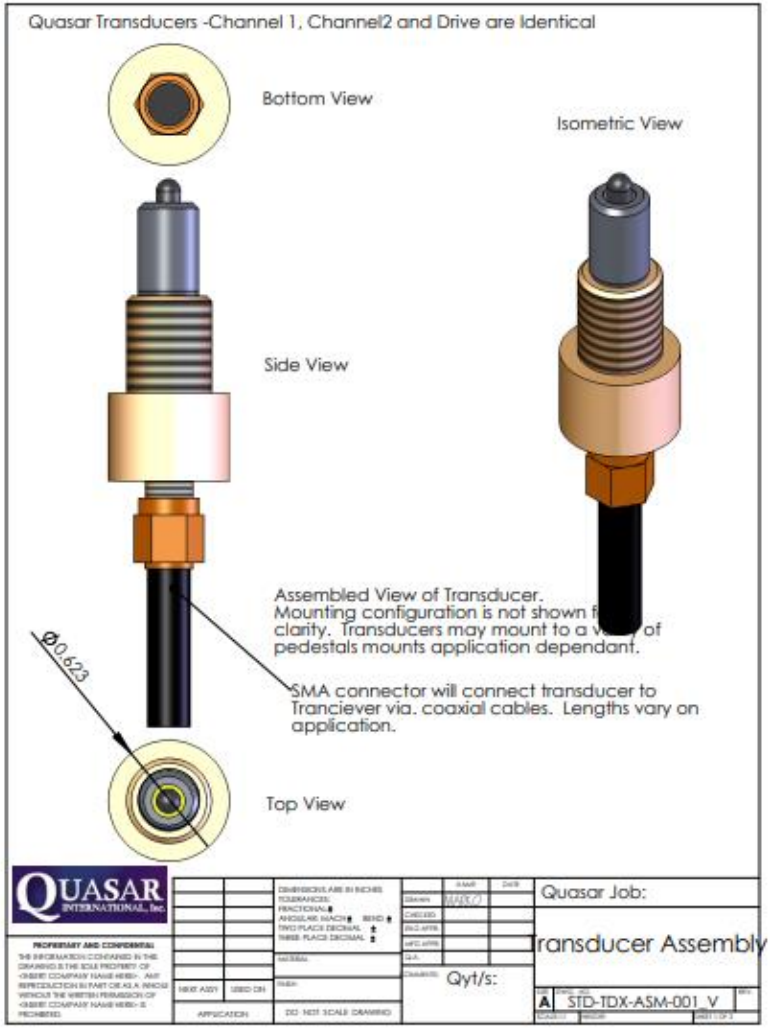

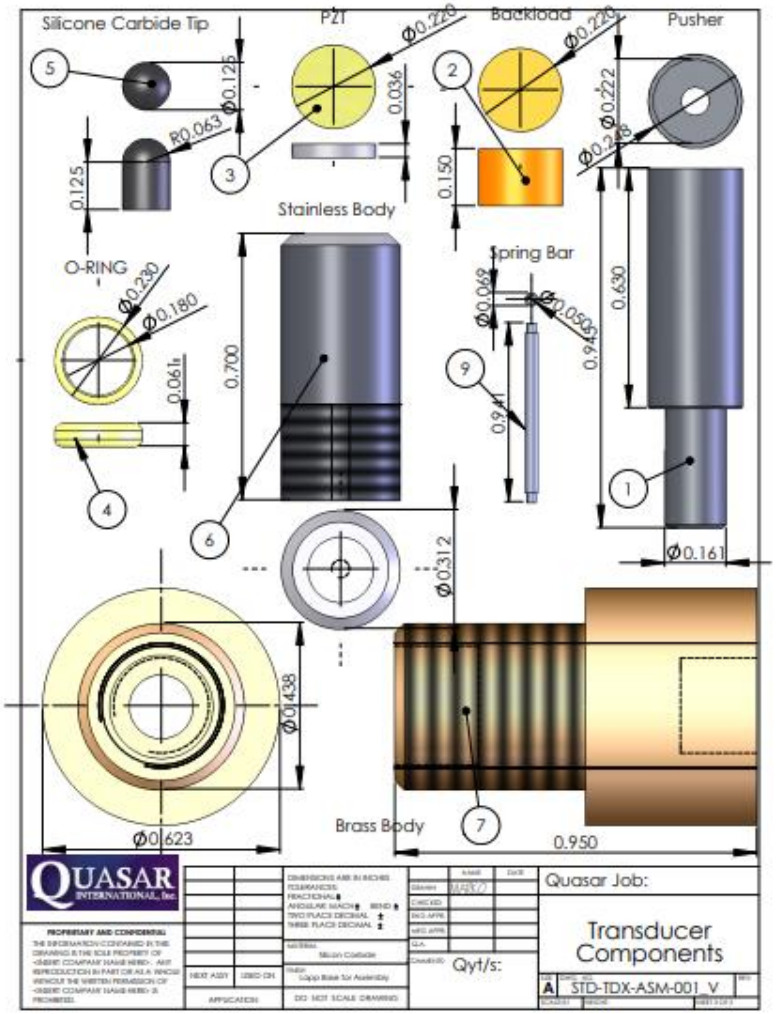

3. Furnace (Micropyretics heaters international)

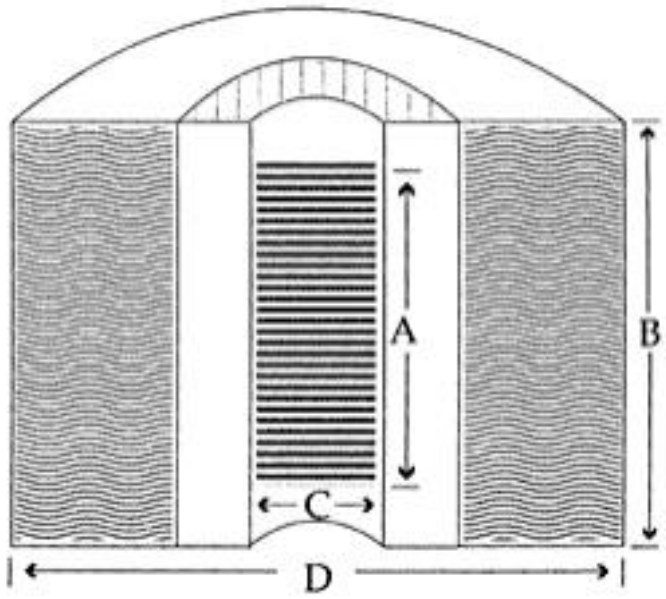

A (Heated Length) = 4″

B (Overall Length) = 6″

C (Internal Diameter) = 2″

D (Outside Diameter) = 6″

4. Transducer holder with cooling system

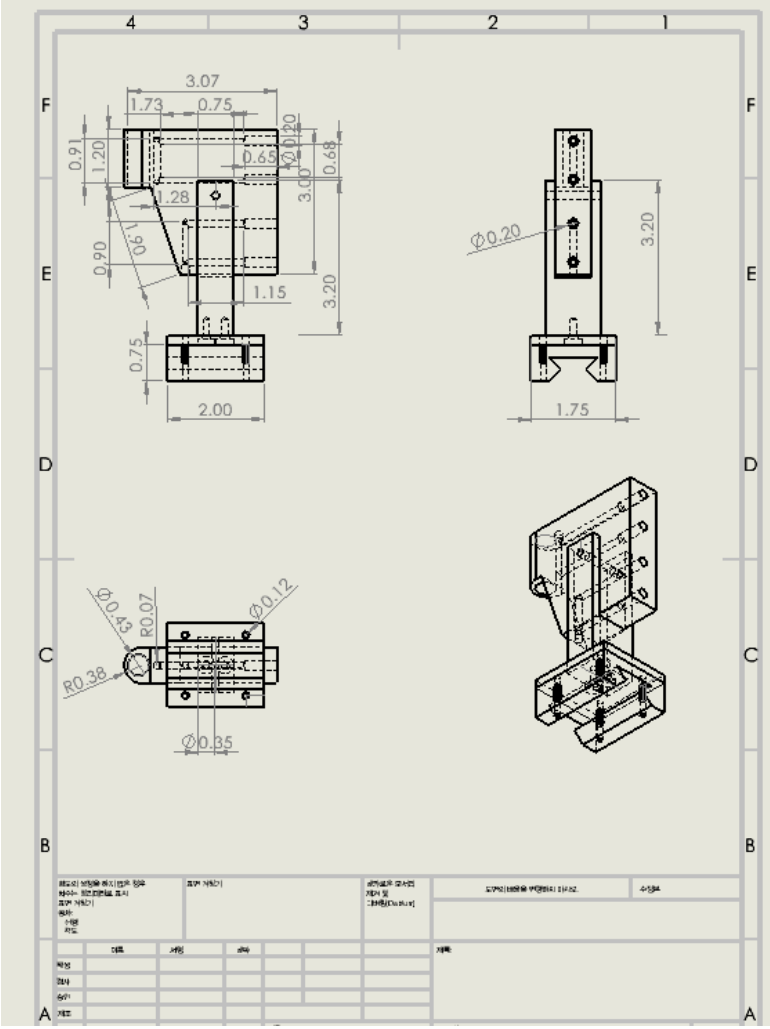

5. Furnace adjustable slide rail

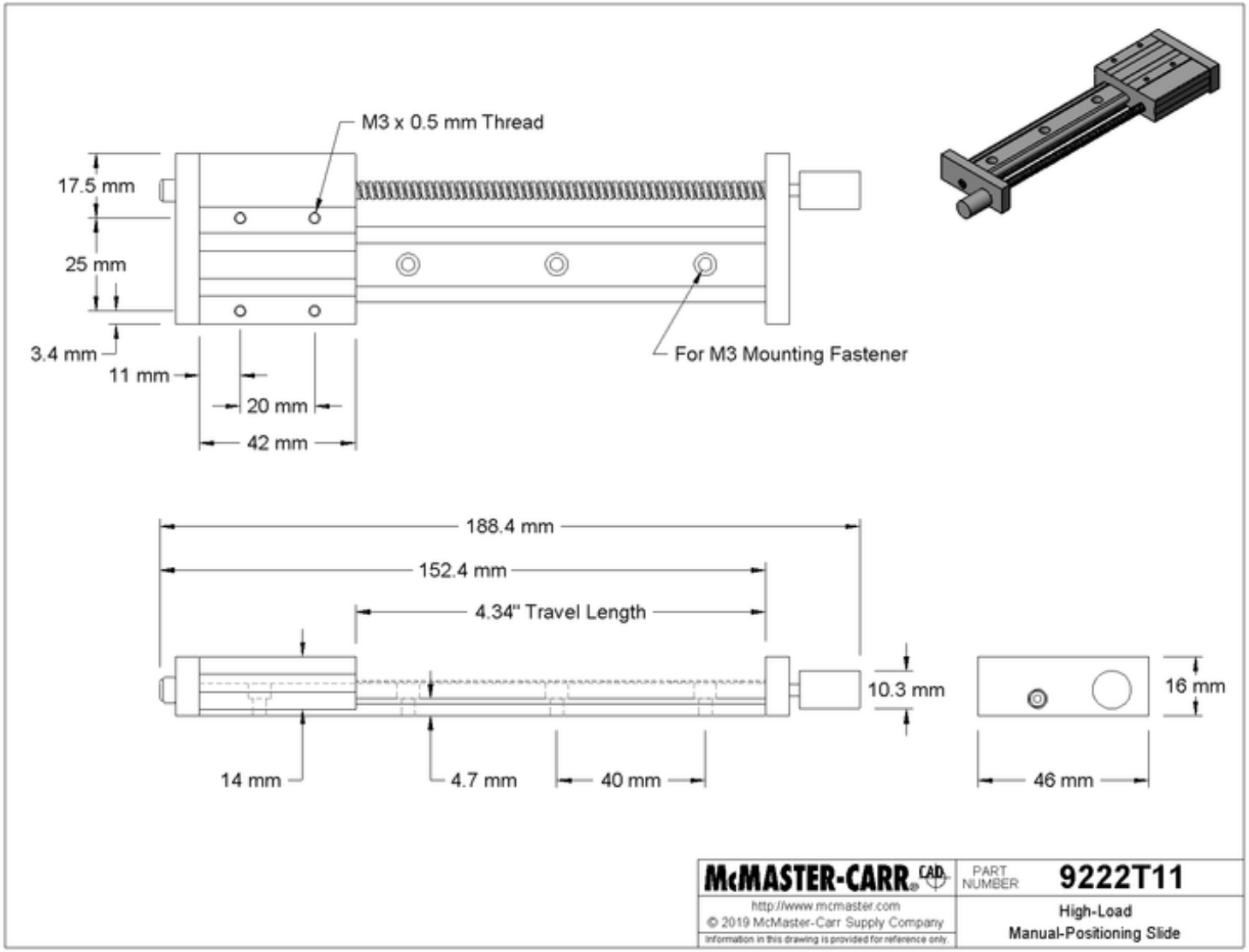

6. Drawer slider on base plate

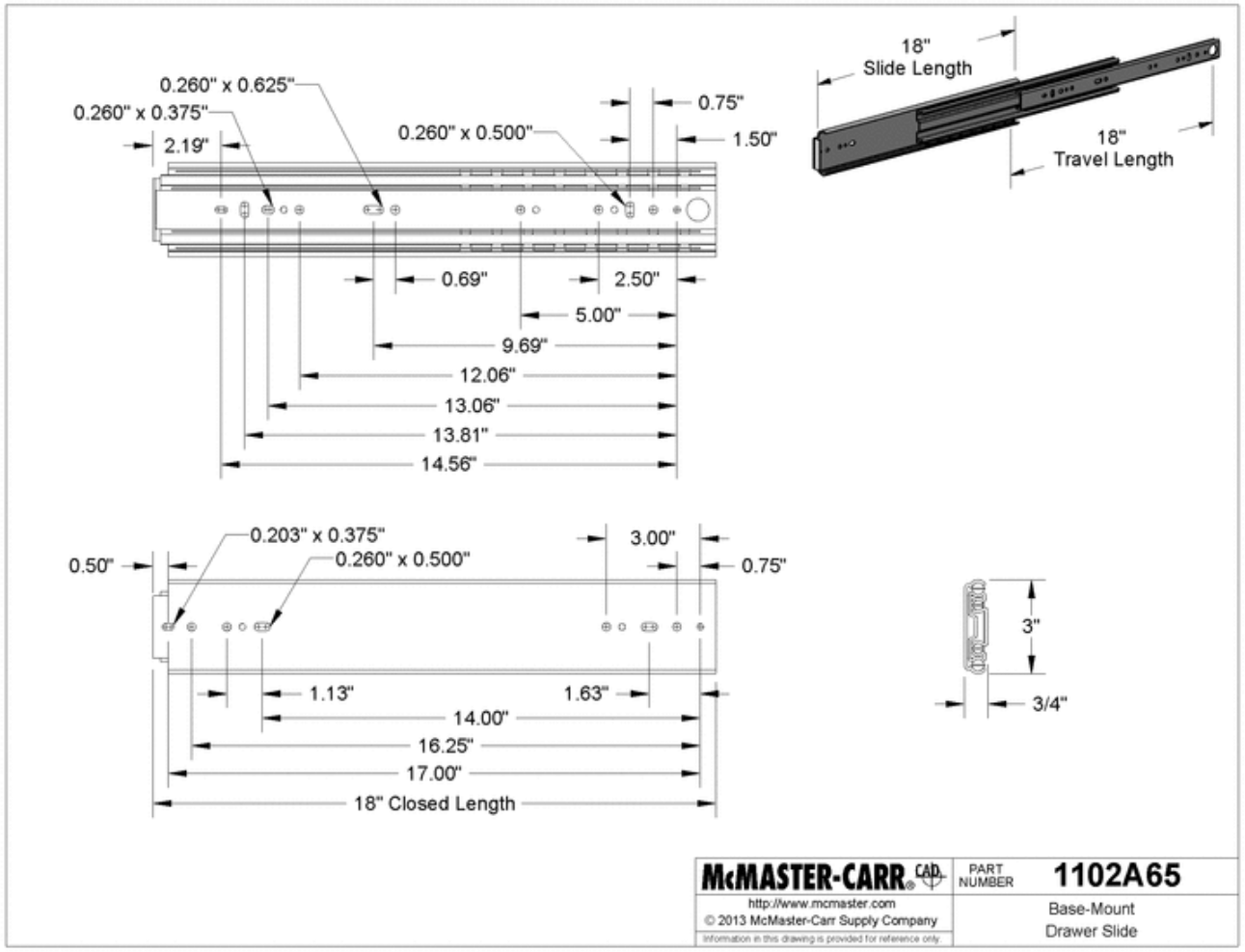

7. The newly developed high temperature RUS of fully assembled tripod stage

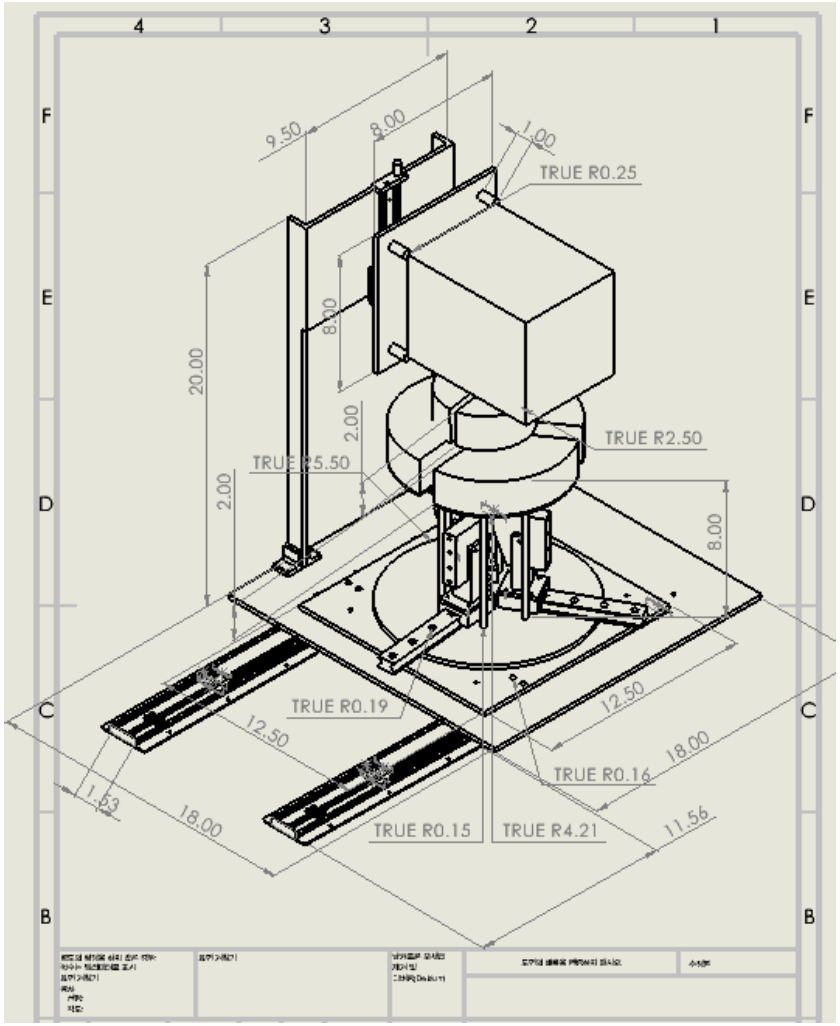

8. Mount table for vacuum chamber

ITEM NO.	DESCRIPTION	QTY.	LENGTH	ANGLE1	ANGLE2	TOTAL LENGTH
1		1				
2	TUBE, SQUARE 2.00 X 2.00 X .25	2	10.49	45°	45°	427.11
3	TUBE, SQUARE 2.00 X 2.00 X .25	4	30	0°	45°	427.11
4	TUBE, SQUARE 2.00 X 2.00 X .25	2	7.41	22.5°	45°	427.11
5	TUBE, SQUARE 2.00 X 2.00 X .25	2	5.66	45°	22.5°	427.11
6	TUBE, SQUARE 2.00 X 2.00 X .25	9	24	0°	0°	427.11
7	TUBE, SQUARE 2.00 X 2.00 X .25	1	28	45°	45°	427.11
8	TUBE, SQUARE 2.00 X 2.00 X .25	4	4	0°	0°	427.11

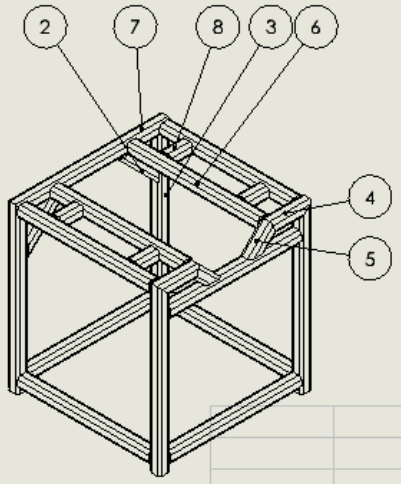

PROPRIETARY AND CONFIDENTIAL
THE INFORMATION CONTAINED IN THIS DRAWING IS THE SOLE PROPERTY OF <INSERT COMPANY NAME HERE>. ANY REPRODUCTION IN PART OR AS A WHOLE WITHOUT THE WRITTEN PERMISSION OF <INSERT COMPANY NAME HERE> IS PROHIBITED.

UNLESS OTHERWISE SPECIFIED:
DIMENSIONS ARE IN INCHES
TOLERANCES:
FRACTIONAL ±
ANGULAR: MACH ± BEND ±
TWO PLACE DECIMAL ±
THREE PLACE DECIMAL ±
INTERPRET GEOMETRIC TOLERANCING PER:
MATERIAL
FINISH
NEXT ASSY | USED ON
APPLICATION | DO NOT SCALE DRAWING

	NAME	DATE
DRAWN		
CHECKED		
ENG APPR.		
MFG APPR.		
Q.A.		
COMMENTS:		

TITLE:
SIZE A | DWG. NO. Furnace Stand | REV
SCALE: 1:16 | WEIGHT: | SHEET 1 OF 1

APPENDIX B

User and maintenance manual

System components:

- Hydra Cool High Vacuum Chamber – Kurt J. Lesker
- Robust Radiator Heating furnace – Micropyretics heaters international
- Chamber bench – Custom made
- Programmable Heating Element Controller – Micropyretics heaters international
- High Temperature RUS Testing Apparatus – Magnaflux
- High Vacuum Turbo pump – Kurt J. Lesker
- Mechanical vacuum pump – Kurt J. Lesker
- Transducer – Magnaflux Quasar
- RUS Platform – Custom made

Components Included with chamber and Testing Apparatus:

- R-type thermocouple (2 pcs.)
- Aluminum Oxide Fiber Insulation (2 pcs.)
- Steel Plate for Test Apparatus (2 pcs.)
- 6 inches single crystal sapphire Rod (3 pcs.)
- Transducers – Magnaflux Quasar (3 pcs.)
- Cooling Water Tubing with Fittings (19 pcs.)
- BNC Cable (from chamber to computer) (3 pcs.)
- Transducer Signal Cable Set (from transducer to chamber)(3 pcs.)
- Transducer holder (3 pcs.)

- Slide Rails (3 pcs.)
- Furnace stand slide (1 pcs.)

High Vacuum Chamber Components and Feed Through:

- Thermocouple Feedthrough R-type and K-type (1 pcs.)
- BNC Cable Feedthrough (1 pcs.)
- Electrical Feedthrough (1 pcs.)
- Liquid/Gas Feedthrough (3 pcs.)
- Vacuum Feedthrough (1 pcs.)
- Pressure gauge Feedthrough (1 pcs.)
- View point (1 pcs.)

High Vacuum Pump Components:

- Gate valve ISO100K (2 pcs)
- Adaptive Reducing Cross ISO-100 to KF-25 (1 pcs)
- Elbow 90 degree NW-100 (2 pcs)
- Bellows vacuum hose KF-25 40 inch (2 pcs)
- Cross 4-Way KF-25 Vacuum Fitting (1 pcs)
- Manual angle valve (3 pcs)
- KF-25 clamp and O-ring (8 sets)
- ISO 100K O-ring (6 pcs)
- Double Claw and Single Claw (48 sets)

Experiment setup assembly

Part A. Transducer holder and stand

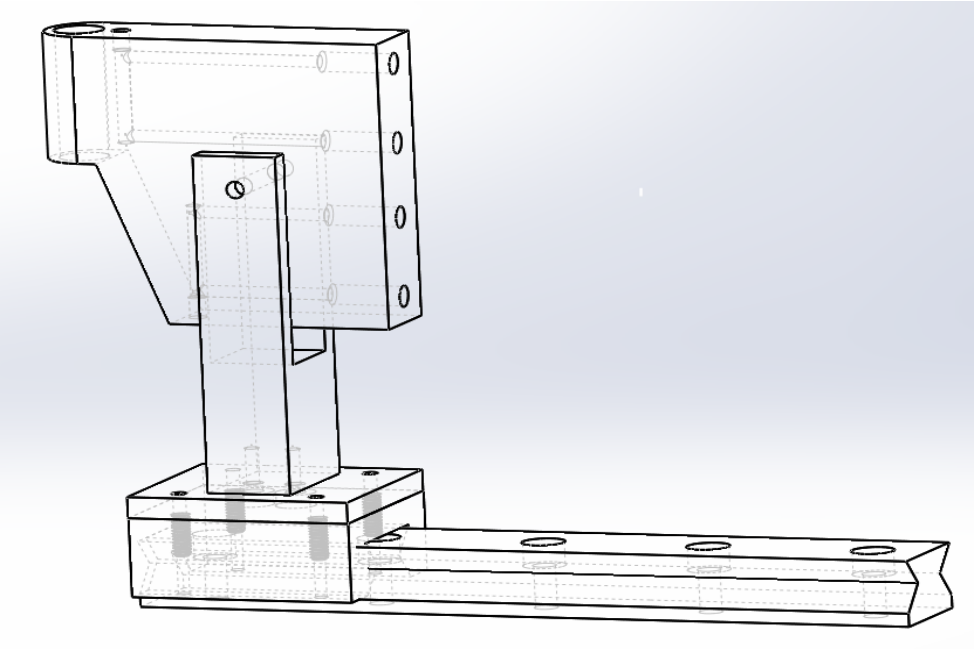

Figure [1]. Transducer stand assembly including base slider.

The first components of the transducer stand is adjustable holder with coolant channeled. The holder with cooling channel will come pre-assembled with four swagelok pipe fittings connected with Polyurethane tubing. A complete assembly can be seen in **Figure [1]**. Seven M4 machine screws are required for assembly as well as additional five M4 screws for base slider to base plate 1. The following is the guideline for assembly of the transducer holder and slider.

● Attach the transducer holder to the stand with a M4 machine screw. The angle of the transducer holder can be adjusted with this set up.

● The slider stand consists of three separate parts: Stand, plate, and the slider base. Attach the stand on to the plate with two screws from the bottom, then attach the plate to the slider base with four screws.

● Once complete, assemble the transducer stand assembly on to the base plate 1, connect Polyurethane coolant hose to the transducer holder. There are four, 3/8 inch threaded entries for swagelok fittings.

● The coolant lines need to be tightened and tested with water to make sure that there is no leak. If there is a large leak, disconnect the fittings and re-apply Teflon tape, and re-connect the fittings to the transducer holder.

● Thread in the transducers carefully into the holder. Note that transducers are very fragile.

● Lastly, Connect the signal cables to transducers.

Part B. Transducer stand assembly and base plate 1

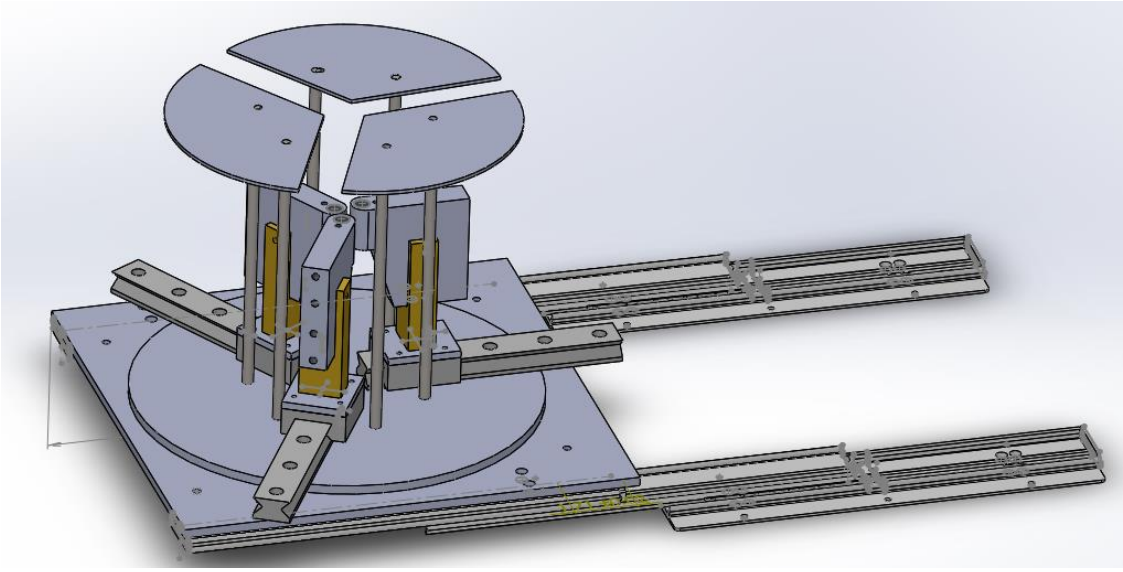

Figure [2]. Complete assembly of transducer stands and support rods with plate including base plate 1

The design consists of three transducer stands and three sets of support rods with plate of insulation and base plate1 with attached drawer sliders. The drawer sliders enable the samples to be conveniently loaded outside of the vacuum chamber. The complete assembly is shown in **Figure [2]**. The following is the guideline of complete assembly of transducer stands and base plate1.

● Attach three transducer stand assemblies on the base plate1 with size M4 screws

● Attach two drawer sliders under the base plate 1 with size M4 screws

● Attach three sets of support aluminum rods on the base plate 1.

Part C. Furnace holder assembly and Furnace with insulations

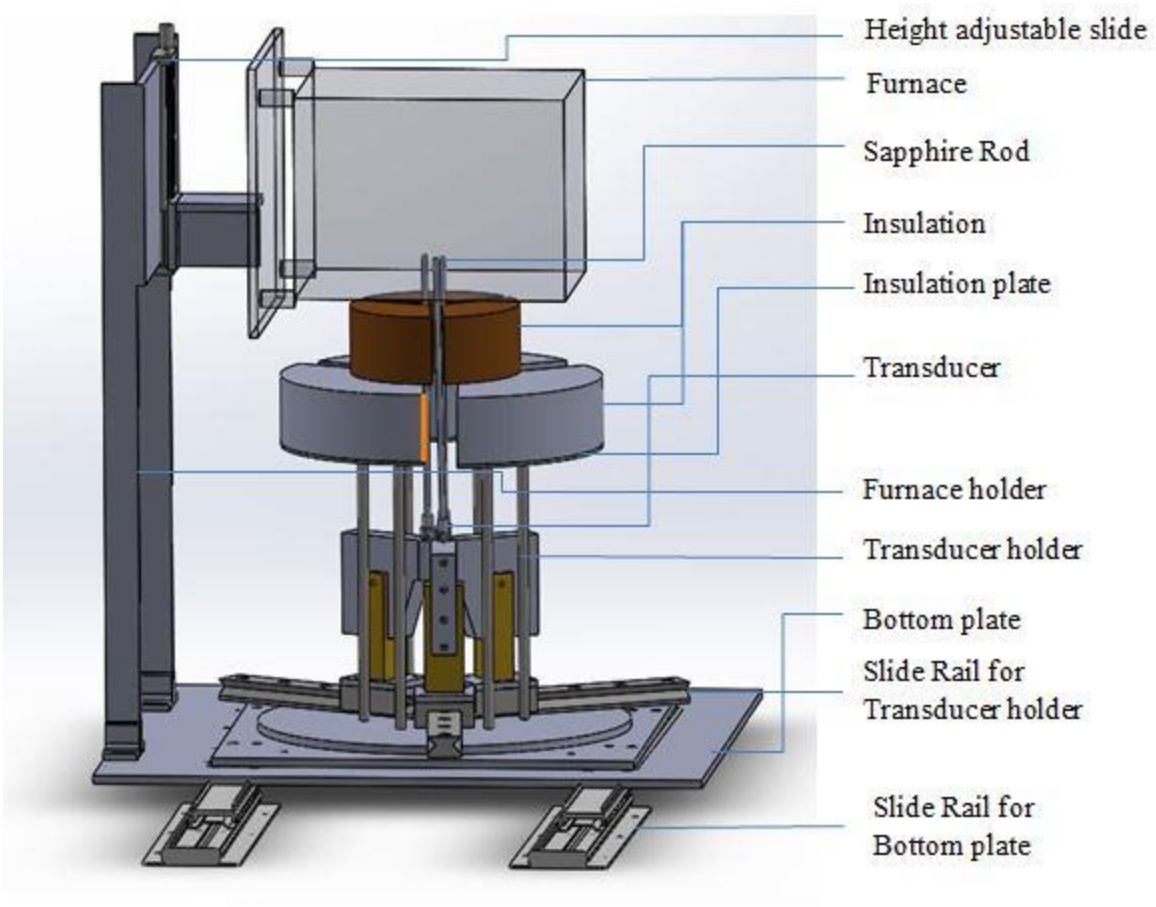

Figure [3]. Complete set up with furnace installed

Furnace holder consists of base plate 2 and a set of 10 inch long stainless steel stands. In order to adjust the height of the furnace, a slider is positioned vertically. Since transducers must maintain under 40℃ while experiment takes place, two layers of alumina insulations are installed under the furnace to minimize heat radiation coming from the furnace. The complete set up is shown in **Figure [3]**. The following is the guideline to complete assembly of the set up.

● Attach four L-shape support components on top of the base plate 2 with M4 screws.

● Two 10 inch stainless steel stands are welded in between L-shape support components.

● Attach the vertical slider with four M4 screws. The total range of vertical distance is about 6 inches up and down.

● Put alumina insulations on top of the support rods plate.

Hydra-cooling Vacuum Chamber

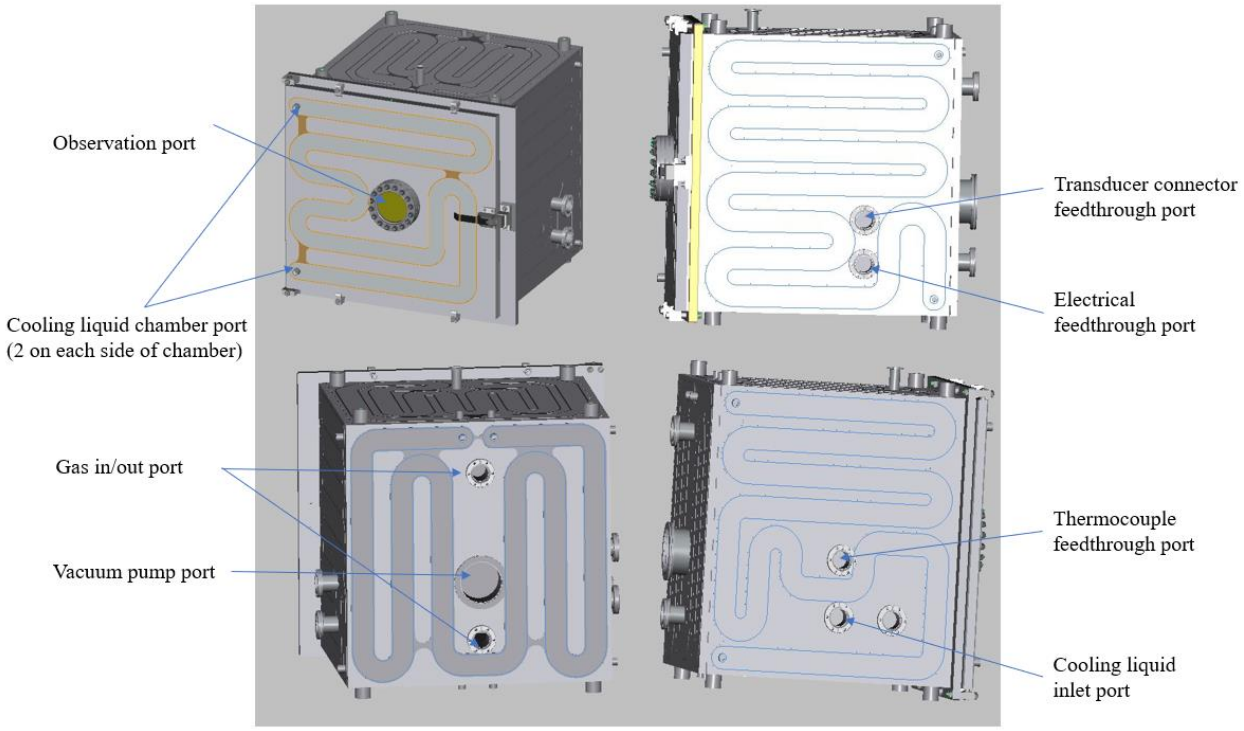

Figure [4] Box chamber assembly with all the ports

To reduce the heat radiation around the furnace inside of the chamber, a liquid cooling path is designed on all 6 sides of the chamber **Figure [4]**. On the front side of the chamber, an observation point is located for viewing inside of the chamber. On the back side of the chamber, Vacuum inlet port and Gas IN/OUT ports are designed. On the right side of the chamber, an electrical feedthrough and single ended transducer connector feedthrough is located. On the left side of the chamber, thermocouple feedthrough as well as cooling liquid inlet and outlet are located. There are a total of 9 ports designed to meet all the connections for the HT-RUS set up. **Figure [4].** The following is a guideline to assemble all the ports with components.

● Two gas feedthrough ports require six 2-1/8 inch hex bolts, six 1/4-28 hex nuts and six 1/4 inch flat washers.

● For the vacuum inlet, attach ISO 100K gate valve with eight double claw clamps and 5/16 inch O-rings

● The liquid feedthrough ports and thermocouple feedthrough port require six of the same sized components as the gas feedthrough ports.

● Transducer connector feedthrough and power feedthrough port require six of the same sized components as the gas feedthrough ports.

● Pressure gauge with hinge clamp and KF-25 O-ring is placed for monitoring the pressure inside of the chamber.

● Install a set of ¼ inch coolant water tubing on each side of the chamber.

Bonding rods on the transducers

Figure [5]. Set up of sapphire rods on to the transducers

The whole set up is shown in the **Figure [5]**. The Blake tubes have inserts that fit one sapphire rod.

● Use Loctite 406 instant adhesive glue on one side of the sapphire Rod.

● Place Rod vertically inside the equipment having the glue side up.

● Place transducers inside of the silver knob. The transducer will make contact with the sapphire rod once the silver knob is threaded into the black tube.

● Wait 24 hours for glue to dry completely then unthread the silver knobs.

● Carefully remove the transducer out of the black tubes.

Note: Use acetone to clean or remove the sapphire rods from the transducers if re-adhesion is needed.

Operating Instructions for RUS

RUSspec is a laboratory system from Magnaflux, which assists in computing elastic constants for various materials including isotropic, cubic, hexagonal, tetragonal, or orthorhombic symmetry. Due to sensitivity to geometry and shape of the specimen, precise samples are required in the form of a rectangular parallelepiped, cylinder, or sphere. Note that a lack of parallelism of only 1% introduces an error of around 10%.

Specimen Preparation

1. Polish every side of the surface of the specimen.
2. Clean the specimen with isopropyl alcohol or ethanol.
3. Measure dimensions of the specimen including thickness, length and width or diameter in several positions and average the data.
4. Obtain average weight of the specimen from multiple measurements.

RUS Setup

1. Connect BNC cables to the connectors on the back of the RUS controller.

2. Slide out the whole RUS assembly outside of the chamber to place the specimen inside the furnace.

3. Place the sample inside of the furnace on the three transducer rods.

4. Put the insulation on top of the furnace and slide back the whole furnace set up carefully inside the chamber. Close the chamber door and secure it.

5. In order to avoid oxidation of the sample at high temperature or to run tests in different environments, first evacuate the chamber to negative 10^{-2}torr by turning on the roughing pump

and opening proper valves on the line to the pump. Specific instructions for valve operation is shown below. Check configuration below shown in **Figure [6]**.

6. Open the gate valve #1 and angle valve #1. Angle valve #2 and gate valve # 2 should be closed.

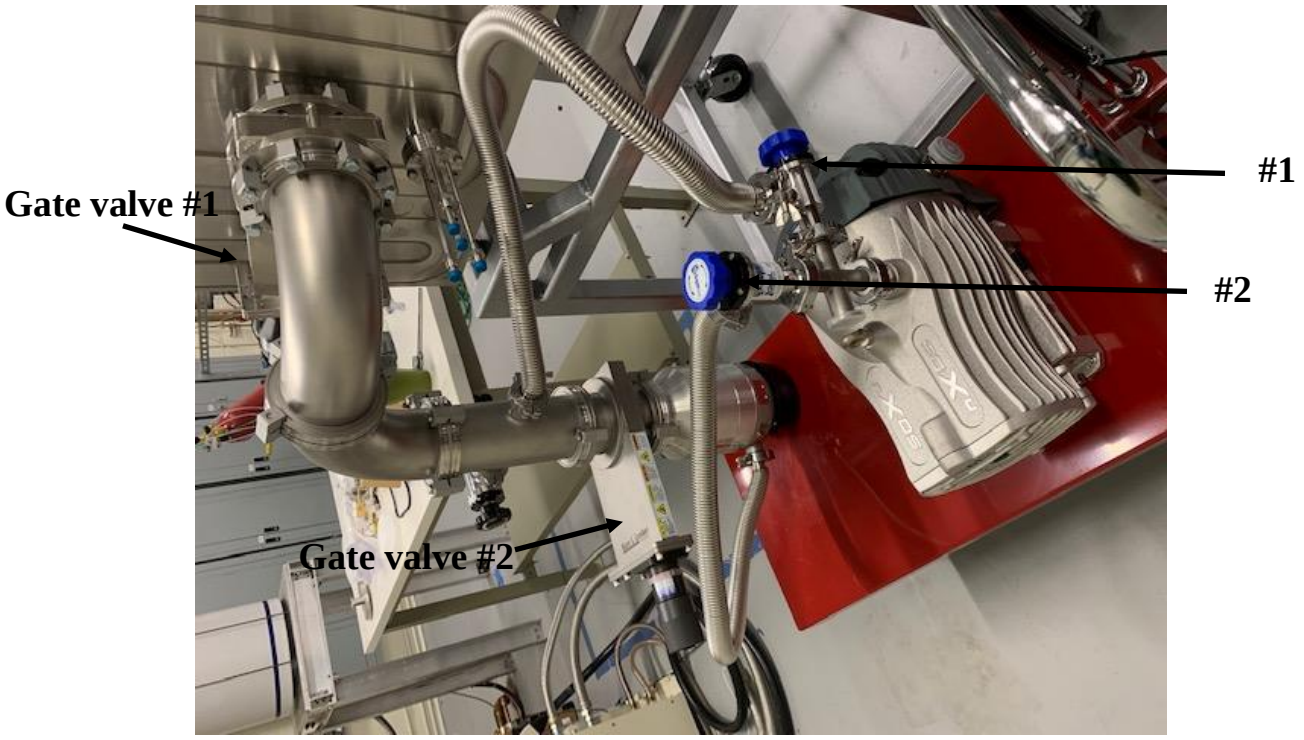

Figure [6]. Vacuum pump connection with all the valves

7. Once the pressure reaches to 10^{-2}torr, close angle valve #1 and turn on the turbopump. Mechanical pump should be on continuously while turbopump is on.

8. Open gate valve #2 and angle valve #2. Wait until pressure reaches to 10^{-5}torr.

9. Once the chamber is evacuated, close all the valves on the line to the vacuum pump and back fill the Chamber with inert gas or any other gas of interest by opening the valve for gas supply. Set the pressure at the gas tank as low as possible (2-3 psi). After some time, cautiously open the valve that leads to the bubbler to check if there is gas flow (See **Figure [7]**). Do not allow water to get sucked into furnace. Open valve only if inert gas pressure activates the bubbler. Adjust valve

position so as not to cause excessive bubbling. Allow gas to escape through bubbler, and then repeat evacuation and backfill at least 3 times.

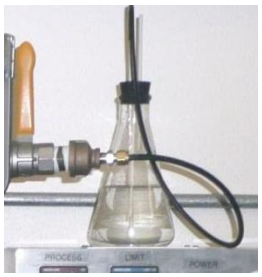

Figure [7]. Bubbler to control flow of inert gas

10. Set desired temperature on temperature controller. See **Figure [8]**. Let system equilibrate 20-30 minutes.

11. Turn on the Chiller. Chiller connection picture and explain

Figure [8]. Temperature controller displays. The target set point is controlled by the process display

12. Open “Quasar RuSpec” software and acquire and save spectrum. (Software instructions explained in next section.

13. Start cooldown by lowering temperature with controllers. Allow inert gas to flow until unit cooled down close to room temperature. Turn off gas, then gas supply to furnace and valve to bubbler and open the chamber.

RUS Data Acquisition

1. Open “Quasar RuSpec” software. Several tabs are located at the top, however, only the “Problem Definition” tab is available until a new model is computed. A screenshot of the software main page is shown in **Figure [9]**.
2. The symmetry of the specimen needs to be specified so that the number of elastic constants that must be entered is visible. If the elastic constants are unknown, a “guess” should be made. Depending on the material types, the number of the constants varies. For example, in isotropic materials the number of the constants is reduced to 2, namely C_{11} and C_{44}.
3. Directly below the symmetry selection, the “# Modes to Calculate” must be addressed; 40-60 modes are recommended. The “Convergence Rate” is usually fixed at 0.5, and the “Polynomial Order” is fixed at 12 to obtain better accuracy.
4. To compute a new model, the geometry of the specimen must be selected among parallelepiped, cylinder, or sphere. Directly above, dimensions in centimeters must be entered. Once the dimensions and mass has been entered, hitting the tab button or clicking in the “density” box, will automatically calculate the density. The “Fit Dimensions” box should be selected for fitting refinement only so that the specimen dimensions are accounted for when calculating the new model.
5. Once all of these parameters have been addressed, click on “Compute New Model”.

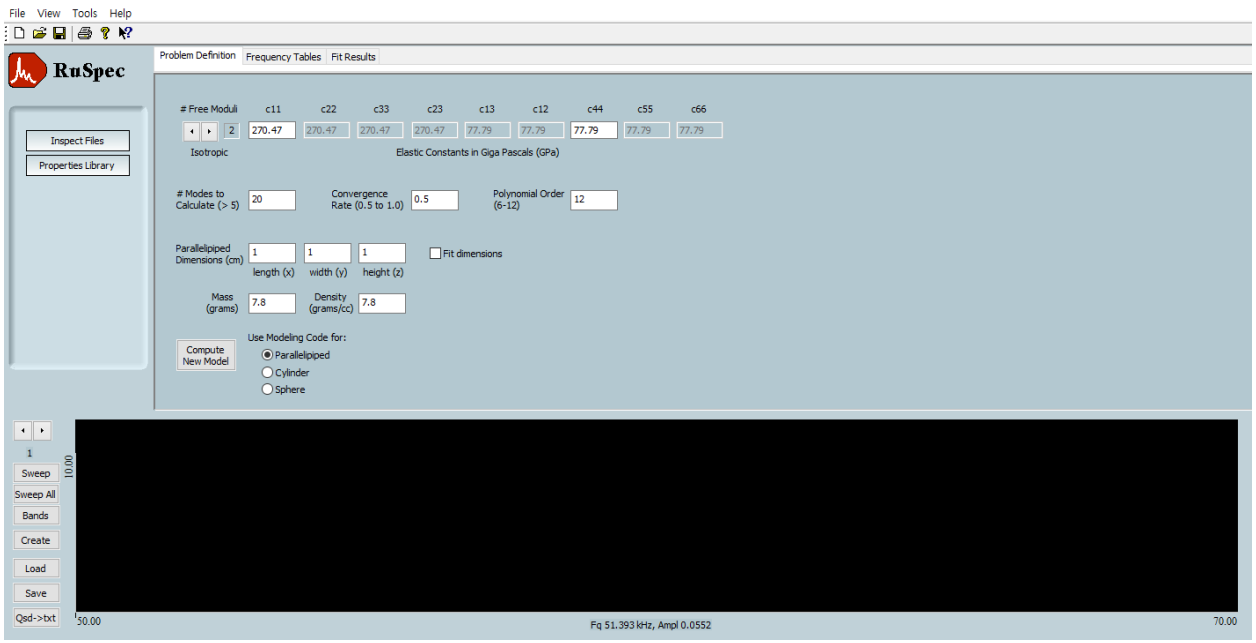

Figure [9]. Screenshot of opening page of Quasar RuSpec software

6. The calculated results will now appear under the “Frequency Tables” tab at the top.
7. A sweep of frequencies must now be used to obtain the actual specimen frequency spectrum.
8. On the bottom left hand side, there is a button labeled “Create” that takes you to the “Setup Bands” box, shown in **Figure [10]**. This allows one to set the starting frequency; the minimum is 10 kHz, and the ending frequency. The “Number of additional Bands” refers to the number of pages the spectrum will be split into for analysis. The “Sample Size” is how many data points will be taken per Hz. The Dwell time is how long each frequency is held at. A spectrum screenshot is shown in **Figure [11]**.

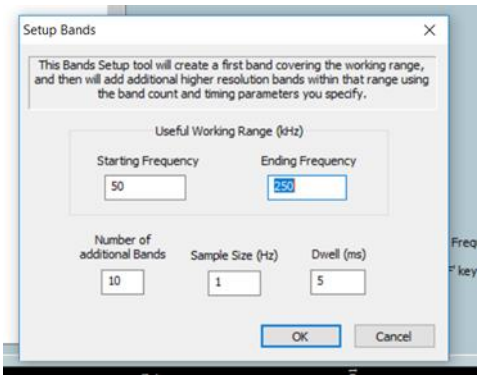

Figure [10]. The "Setup Bands" box for configuring the frequency sweep.

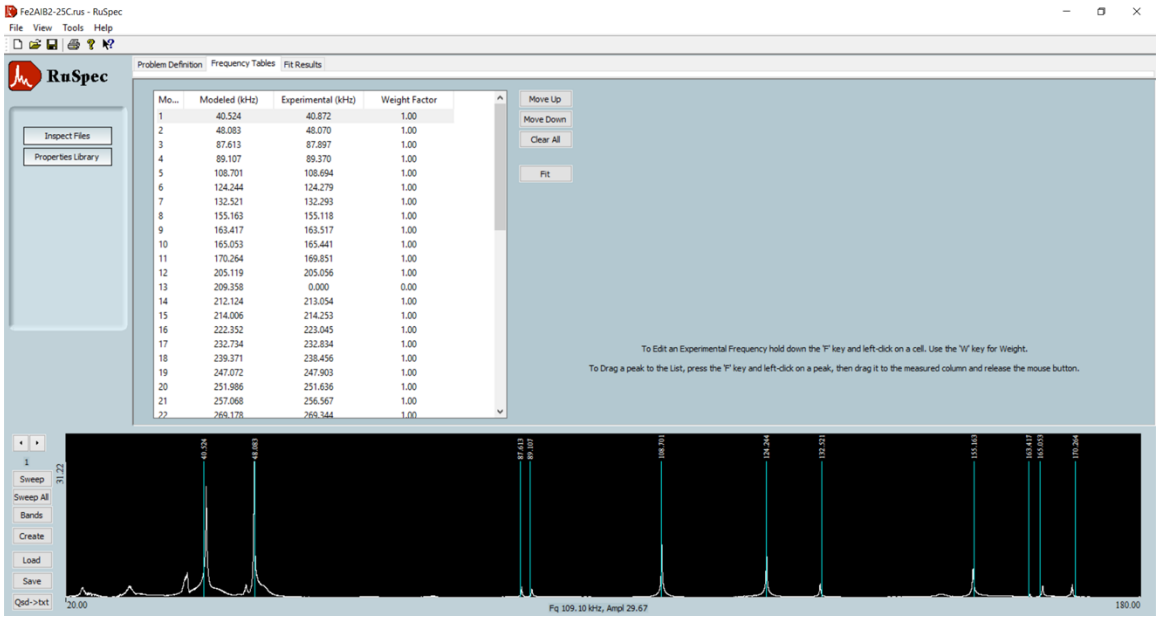

Figure [11]. Sample spectrum for specimen of a boride ceramics. Band from 20 to 180 kHz

9. ***The spectrum should immediately be saved*** using the "Save" button on the bottom left. The spectrum can be converted into a text file using the "Qsdtxt" button.
10. The experimental frequencies need to be inputted into the frequency table. To do this, draw a box over the frequency peak that seems closest to the Modeled frequency. At the Shift + Click over the center of the peak.
11. The "Weight Factor" column is used so that a specific mode is fitted or not. A weight factor of 1.0 is the highest factor and should be used for all experimental peaks that are selected. If

a modeled peak does not fit with an experimental value, the default weight will be left at zero.

12. Once all peaks have been correctly placed under “Experimental”, click the button “Fit” on the right side of the table.
13. After the software fits the results, the next screen that appears (shown in **Figure [12]**) will contain a better approximation of the elastic constants, the RMS error, and properties such as Young’s Modulus, Shear Modulus, Bulk Modulus, and Poison’s Ratio. Note that an RMS error of 0.5% of less can be acceptable.

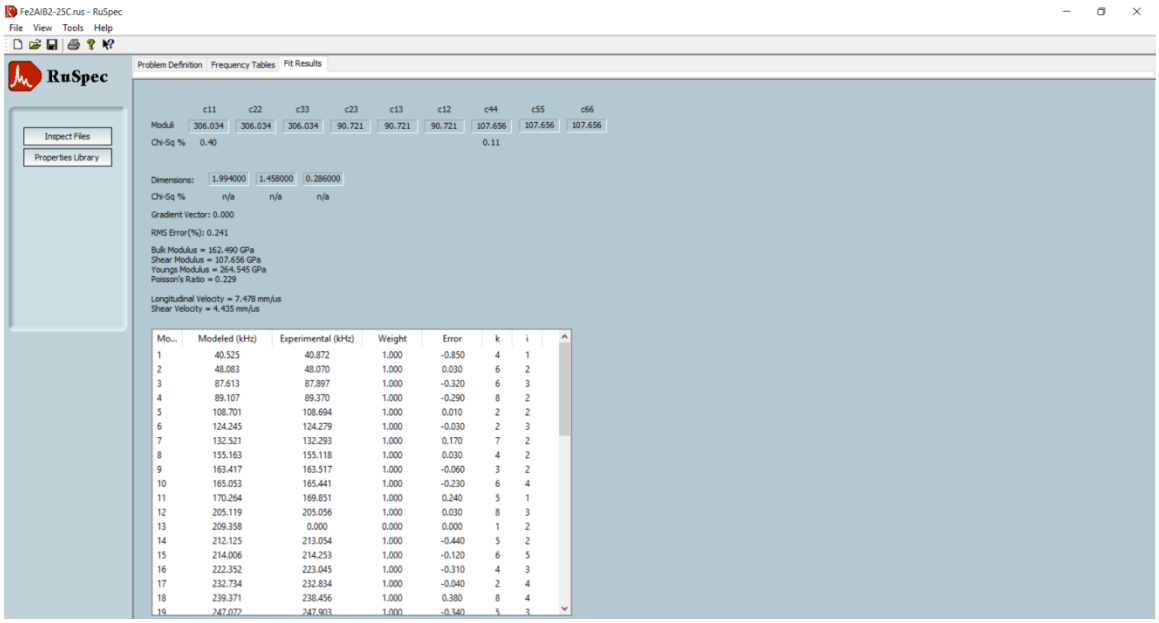

Figure [12]. Screen and data obtained after fitting results